

RESEARCH ARTICLE

A polymorphic residue that attenuates the antiviral potential of interferon lambda 4 in hominid lineages

Connor G. G. Bamford¹, Elihu Aranday-Cortes¹, Ines Cordeiro Filipe¹, Swathi Sukumar¹, Daniel Mair¹, Ana da Silva Filipe¹, Juan L. Mendoza², K. Christopher Garcia², Shaohua Fan³, Sarah A. Tishkoff³, John McLauchlan^{1*}

1 MRC-University of Glasgow Centre for Virus Research, Glasgow, United Kingdom, **2** Howard Hughes Medical Institute, Department of Molecular and Cellular Physiology and Department of Structural Biology, Stanford University School of Medicine, Stanford, CA, United States of America, **3** Departments of Genetics and Biology, University of Pennsylvania, Philadelphia PA, United States of America

* john.mclauchlan@glasgow.ac.uk



OPEN ACCESS

Citation: Bamford CGG, Aranday-Cortes E, Filipe IC, Sukumar S, Mair D, Filipe AdS, et al. (2018) A polymorphic residue that attenuates the antiviral potential of interferon lambda 4 in hominid lineages. *PLoS Pathog* 14(10): e1007307. <https://doi.org/10.1371/journal.ppat.1007307>

Editor: Glenn Randall, The University of Chicago, UNITED STATES

Received: May 16, 2018

Accepted: August 29, 2018

Published: October 11, 2018

Copyright: © 2018 Bamford et al. This is an open access article distributed under the terms of the [Creative Commons Attribution License](https://creativecommons.org/licenses/by/4.0/), which permits unrestricted use, distribution, and reproduction in any medium, provided the original author and source are credited.

Data Availability Statement: All relevant data are within the paper and its Supporting Information files.

Funding: JLM is supported by National Institutes of Health (<https://www.nih.gov/>) award K01CA175127. SF and SAT were supported by National Institutes of Health (<https://www.nih.gov/>) grants 1R01DK104339-0 and 1R01GM113657-01. This work was funded by the UK Medical Research Council (<https://mrc.ukri.org/>) (MC_UU_12014/1). The funders had no role in study design, data

Abstract

As antimicrobial signalling molecules, type III or lambda interferons (IFNλs) are critical for defence against infection by diverse pathogens, including bacteria, fungi and viruses. Counter-intuitively, expression of one member of the family, IFNλ4, is associated with decreased clearance of hepatitis C virus (HCV) in the human population; by contrast, a natural frameshift mutation that abrogates IFNλ4 production improves HCV clearance. To further understand how genetic variation between and within species affects IFNλ4 function, we screened a panel of all known extant coding variants of human IFNλ4 for their antiviral potential and identify three that substantially affect activity: P70S, L79F and K154E. The most notable variant was K154E, which was found in African Congo rainforest ‘Pygmy’ hunter-gatherers. K154E greatly enhanced *in vitro* activity in a range of antiviral (HCV, Zika virus, influenza virus and encephalomyocarditis virus) and gene expression assays. Remarkably, E154 is the ancestral residue in mammalian IFNλ4s and is extremely well conserved, yet K154 has been fixed throughout evolution of the hominid genus *Homo*, including Neanderthals. Compared to chimpanzee IFNλ4, the human orthologue had reduced activity due to amino acid K154. Comparison of published gene expression data from humans and chimpanzees showed that this difference in activity between K154 and E154 in IFNλ4 correlates with differences in antiviral gene expression *in vivo* during HCV infection. Mechanistically, our data show that the human-specific K154 negatively affects IFNλ4 activity through a novel means by reducing its secretion and potency. We thus demonstrate that attenuated activity of IFNλ4 is conserved among humans and postulate that differences in IFNλ4 activity between species contribute to distinct host-specific responses to—and outcomes of— infection, such as HCV infection. The driver of reduced IFNλ4 antiviral activity in humans remains unknown but likely arose between 6 million and 360,000 years ago in Africa.

collection and analysis, decision to publish, or preparation of the manuscript.

Competing interests: The authors have declared that no competing interests exist.

Author summary

Natural genetic variation and its influence on the outcome of viral infection is a topical area given the wealth of genetic data now available. However, understanding how clinical phenotype is affected by genetic variation at the molecular level is often lacking yet critical for any insight into immunity and disease. It is known that variants in the antiviral ‘interferon lambda 4’ (*IFNL4*) gene significantly influence outcome of hepatitis C virus (HCV) infection in humans. Counter-intuitively, those producing *IFNL4* have greater risk of establishing chronic HCV infection, compared to individuals with an inactive variant, although the underlying mechanisms remain poorly understood. From a comprehensive screen of all natural human variants, we show that the most common form of IFNλ4 is less able to protect human cells from pathogenic virus infection than the equivalent protein from our closest living relative the chimpanzee. This is as a result of a single amino acid substitution that impedes its release from cells and reduces antiviral gene expression. Our observed differences in activity correlated with divergent host responses in HCV-infected livers from humans and chimpanzees. We suggest that human *IFNL4* evolution places humans at a disadvantage when infected with pathogens such as HCV.

Introduction

Vertebrates have evolved the capacity to coordinate their antiviral defences through the action of proteins called interferons (IFNs) [1], which are small secreted signalling proteins produced by cells after sensing viral infection. IFNs bind to cell surface receptors, commencing autocrine and paracrine signalling via the ‘JAK-STAT’ pathway. Through this mechanism, IFNs induce expression of hundreds of ‘interferon-stimulated genes’ (ISGs) that establish a cell-intrinsic ‘antiviral state’ and regulate cellular immunity and inflammation [2,3]. Thus, IFNs are pleiotropic in activity and modulate aspects of protective immunity and pathogenesis [4].

Three groups of IFNs have been identified (types I–III), with the type III family (termed IFNλs) being the most recently discovered [5,6]. Emerging evidence highlights the critical and non-redundant role that IFNλs play in protecting against diverse pathogens, including viruses, such as norovirus [7], influenza virus [8] and flaviviruses [9]; bacteria [10]; and fungi [11]. While IFNλs induce nearly identical genes to type I IFNs, differences in signalling kinetics and cell-type specificity contribute to their specialisation [12,13]. Hence, as a consequence of selective expression of the IFNλ receptor 1 (IFNλR1) co-receptor on epithelial cells [13], type III IFNs play a significant role in defence of ‘barrier tissues’, such as the gut, respiratory tract and liver [reviewed in 14]; the second co-receptor for IFNλ is IL10-R2, which is expressed more broadly.

Although important for host defence, some IFNs are highly polymorphic [15]. In humans, a number of genetic variants in the type III IFN locus (containing IFNλs 1–4) have been identified and are associated with clinical phenotypes relating to viral infection [16–18]. Although many of these variants are in linkage disequilibrium, the major functional variant is thought to lie in the *IFNL4* gene [19]. This causative variant is a single substitution/insertion mutation converting the ‘ΔG’ allele to a ‘TT’ allele (rs368234815), thereby yielding a frameshift which leads to loss of active human IFNλ4 (HsIFNλ4) [18]. Genome-wide association studies have convincingly demonstrated a seemingly counter-intuitive correlation between the *IFNL4* ΔG allele and reduced clearance of hepatitis C virus (HCV) infection, i.e individuals who produce HsIFNλ4 clear HCV infection with reduced frequency in the presence or absence of antiviral IFN therapy [17,18]. Although IFNλ4 is highly conserved among mammals, the ‘pseudogenising’ TT allele of

HsIFN λ 4 has evolved under positive selection in some human populations suggesting that expression of the wild-type protein likely conferred a fitness cost during recent human evolution [20]. Expression of IFN λ 4 is tightly controlled and reduced in human as well as Gorilla cells following viral infection compared to IFN λ 3 [21]. The mechanism underlying the contribution of HsIFN λ 4 to viral persistence in HCV infection is not well understood but is associated with enhanced ISG induction. Moreover, a common natural variant of HsIFN λ 4 (P70S) [18], which has reduced signalling capacity, is also linked with improved HCV clearance [22]. Thus, there is a spectrum of HsIFN λ 4 activity in humans as a consequence of natural variation that has a significant influence on chronic HCV infection, with wt HsIFN λ 4 representing the protein with apparently the greatest antiviral activity.

Whether other human IFN λ 4 variants exist in addition to P70S, which affect antiviral activity, has not been explored fully. In this study, we have examined human genetic data to identify other possible naturally occurring IFN λ 4 variants and performed comparative analysis with mammalian orthologues in species closely related to humans. We provide evidence that the antiviral potential for the most common form of IFN λ 4 in humans has attenuated activity due to a single amino acid substitution. In addition, we propose that acquisition of the attenuating substitution arose very early during human evolution but that some populations do encode a more active variant. Mechanistically, our data show that the reduced antiviral potential of human IFN λ 4 results from a likely dual defect in secretion and potency.

Results

Functional consequences of human IFN λ 4 non-synonymous variation

Firstly, we undertook genetic and functional comparisons of natural human IFN λ 4 coding variants present in the human population. We identified 15 non-synonymous HsIFN λ 4 variants in the 1000 Genomes Project Database [23] (Fig 1A and S1 Data), including three previously described variants (C17Y, P60R and P70S; >1% global frequency, classified as ‘common’) [18]. The remaining 12 variants were classified as rare (<1% global frequency). The African population harboured the largest number of, as well as the most unique, variants. Interestingly, three rare variants (A8S, S56R and L79F) were shared exclusively between African and American populations, which may have arisen due to relatively recent movements of people perhaps through the transatlantic slave trade.

Variants were located in regions of functional significance in the HsIFN λ 4 protein (Fig 1B and S1A–S1C Fig), such as the predicted signal peptide (amino acids 1–24), surrounding the single glycosylation site (N61) [both of which are required for secretion of active protein], and helix F that is predicted to interact with the IFN λ R1 receptor (variants 151–158) [24]. Interestingly, the variants in helix F were clustered in the N-terminal portion of the predicted helix. Based on the above predictions, we hypothesised that some of these variants may have phenotypic effects on HsIFN λ 4 function. Of note, no variants were found in helix D, which is predicted to contribute to interaction with the IL-10R2 receptor, nor on the IL-10R2-interacting face of the protein.

The functional impact of variation on HsIFN λ 4 has only been assessed for the common P70S variant and so we sought to screen all other variants in activity assays. To determine whether variants affected HsIFN λ 4 antiviral activity, they were introduced independently into an expression plasmid that produced HsIFN λ 4 with a C-terminal ‘FLAG’ tag. Transient transfection of the expression plasmids into human ‘producer’ cells (HEK-293T cells) allowed harvesting of active HsIFN λ 4 in the cell supernatant (referred to herein as conditioned media [CM]) thereby enabling analysis of the effects of variants on HsIFN λ 4 production, glycosylation, secretion and potency; a similar approach has been successfully adopted previously to

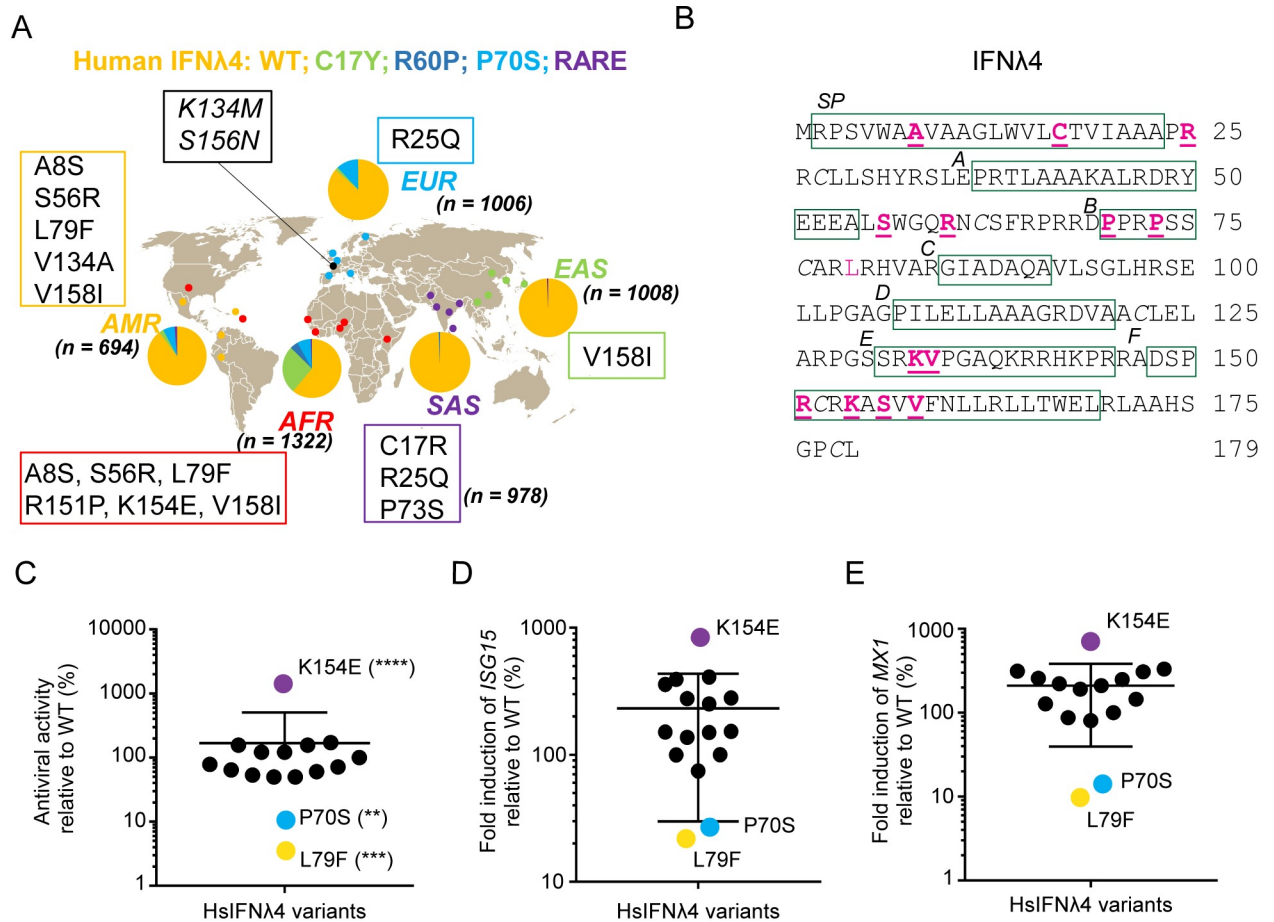


Fig 1. Rare non-synonymous variants of HsIFNλ4 affect antiviral activity. (A) Ancestry-based localization and frequency of human non-synonymous variants of HsIFNλ4 in African (AFR), South Asian (SAS), East Asian (EAS), European (EUR) and American (AMR) populations within the 1000 Genomes Database. ‘n’ represents the number of alleles tested in each population. Common and rare variants are those which have frequencies of >1% and <1% respectively in the 1000 Genome data. Common variants include: wt (orange), C17Y (light green), R60P (dark blue) and P70S (cyan). Rare variants (purple) include: A8S, C17R, R25Q, S56R, P73S, L79F, K133M, V134A, R151P, K154E, S156N, and V158I. Variants K133M and S156N (black) did not have an associated ethnicity but were found in the dataset from the Netherlands (Genome of the Netherlands cohort) [72]. (B) Location of non-synonymous variants in the HsIFNλ4 polypeptide (underlined pink). Regions of predicted structural significance are boxed (green), including the signal peptide (SP) and helices (A to F) [24]. There is a single N-linked glycosylation site at position 61 (N61). Note that there are 2 non-synonymous changes at C17 (C17R and C17Y). Cysteine residues involved in disulphide bridge formation are italicised. See S1 Data for genetic identifiers for the variants described here. (C) Antiviral activity of all HsIFNλ4 natural variants in an anti-EMCV CPE assay relative to wt protein in HepaRG cells. Cells were stimulated with serial dilutions of HsIFNλ4-containing CM for 24 hrs and then infected with EMCV (MOI = 0.3 PFU/cell) for 24 hrs at which point CPE was assessed by crystal violet staining. After staining, the dilution providing ~50% protection was determined. Mean of combined data from three independent experiments performed on different days (n = 3) are shown. Error bars represent mean and SEM for all variants combined. Data are shown in S2A Fig. **** = <0.0001; *** = <0.001; ** = <0.01 by one-way ANOVA compared to wt with a Dunnett’s test to correct for multiple comparisons. Controls (HsIFNλ4-TT and EGFP) are shown in S2 Fig and gave no protection against EMCV in the assay. Those variants with >2-fold change are highlighted with colours: purple (K154E), cyan (P70S) and yellow (L79F). (D and E) ISG gene expression determined by RT-qPCR following stimulation of cells with HsIFNλ4 variants. Relative fold change of ISG15 (D) and Mx1 mRNAs (E) in HepaRG cells stimulated with CM (1:4 dilution) from plasmid-transfected cells compared to wt HsIFNλ4. Cells were stimulated for 24 hrs. Data points show mean of biological replicates (n = 3) and the error bar represents mean and SEM for all variants combined. Expanded data are shown in S2B and S2C Fig. Variants are coloured based on antiviral assays described in Fig 1C.

<https://doi.org/10.1371/journal.ppat.1007307.g001>

determine the relative activities of secreted HsIFNλ3 and HsIFNλ4 as well as a HsIFNλ4 variant that is not glycosylated [24]. We chose to screen the function of the panel of HsIFNλ4 variants on the interferon-competent hepatocyte cell line HepaRG cells [25].

Firstly, we investigated the antiviral activity of variants by titrating them against encephalomyocarditis virus (EMCV), a highly IFN-sensitive and cytopathic virus used to measure IFN-

mediated protection [26] (**Fig 1C and S2A Fig**). We also measured their capacity to induce two major ISGs, *MX1* and *ISG15*, by RT-qPCR (**Fig 1D and 1E and S2B and S2C Fig**) and validated the *ISG15* mRNA data by determining production of unconjugated 'mono' *ISG15* and high-molecular weight *ISG15*-conjugates ('ISGylation'; **S2D Fig**). In addition, we constructed a series of negative controls (plasmids expressing EGFP and the frameshift TT variant of HsIFN λ 4), a positive control (HsIFN λ 3op) for comparative analysis to examine HsIFN λ 4 activity, and three HsIFN λ 4 variants, which do not occur naturally but were included as they could alter post-translational modification (N61A which ablates glycosylation) or potential receptor interactions (F159A and L162A located in helix F), respectively [27]. Negative controls (EGFP or the frameshift TT variant) gave very low induction of *ISG15* and *MX1* and no detectable antiviral activity in the EMCV assay whereas the positive control (HsIFN λ 3op) was highly active in both assays (**S2A–S2C Fig**). The non-natural variants N61A and F159A almost abolished activity compared to wt HsIFN λ 4 and HsIFN λ 3op while L162A gave slightly less activity in the ISG induction assay but activity was reduced to a greater extent in the EMCV assay. In a previous report, ablating glycosylation at N61 substantially reduced activity of secreted HsIFN λ 4 in an ISG induction assay [24]. Thus, our assay systems recapitulated findings from previous studies with similar assays and provided a range of activities to assess the impact of the natural HsIFN λ 4 variants.

Our analyses on the natural HsIFN λ 4 variants revealed that only three variants (P70S, L79F and K154E) consistently and substantially modulated antiviral activity and signalling compared to wt HsIFN λ 4 (**Fig 1C–1E**). The impact of these variants was particularly pronounced in the EMCV assay that measures the dilution giving 50% activity over a large range of dilutions (**Fig 1C**). Our results confirmed previous observations on the lower activity of the P70S variant [22] and demonstrated that the rare L79F variant had a similar phenotype. By contrast, the K154E variant substantially enhanced antiviral activity and ISG induction.

These effects on activity for P70S, L79F and K154E did not arise from differences in the levels of HsIFN λ 4 intracellular production or changes to glycosylation (**S3A and S3B Fig**). However, variants S56R and R60P (R60P is a common variant in Africa) did lead to marked reductions in the glycosylated form of HsIFN λ 4 as demonstrated by the mean ratio of glycosylated:non-glycosylated protein (**S3 Fig**) but did not greatly alter their antiviral activity in contrast with our findings with the N61A non-natural variant, which abolished both glycosylation and antiviral activity of conditioned media (**S2A–S2C Fig and S3A and S3B Fig**). From this screen, we concluded that three non-synonymous variants in HsIFN λ 4 (P70S, L79F and K154E), identified as either common or rare alleles in the human population, affect the antiviral activity of the protein.

Examining the global distribution of genetic variation can help understand its origins, evolution and functional consequences. P70S is a common variant that is found worldwide (in every population in the 1000 Genomes Database). By contrast, L79F and K154E are rare and, based on evidence in the 1000 Genomes Project Database, geographically restricted to West Africa/Americas, and central Africa, respectively (**Fig 1A**). We were able to obtain DNA from lymphoblastoid cell lines developed from the 2 individuals encoding the L79F variant; our analysis revealed that the West African subject carried the SNP for this variant but not the individual from the Americas see **Materials and Methods**). Thus, we could verify the occurrence of the L79F variant in Africa but not in the Americas. From further interrogation of the 1000 Genomes Database [28], the HsIFN λ 4 K154E variant was present in two individuals from different African rainforest 'Pygmy' hunter-gatherer populations (Baka and Bakola) in Cameroon (**S4A Fig**). The Bakola individual was homozygous for the Δ G allele, indicating that the K154E variant would be encoded on one of the functional Δ G HsIFN λ 4 alleles. The Baka subject was heterozygous at rs368234815 (Δ G/TT) and thus only one allele (Δ G) would

produce full-length HsIFN λ 4, presumably K154E. The other allele (TT) is a pseudogene and would not lead to expression of functional HsIFN λ 4. Each of the Baka and Bakola individuals also had additional non-synonymous HsIFN λ 4 variants (V158I and R151P, Baka and Bakola individuals respectively); these variants were included in our functional screen of HsIFN λ 4 variants but did not significantly alter activity (Fig 1C–1E and S2A–S2C Fig). From analysis of the Genome Aggregation Database (gnomAD) [29], the SNP variant resulting in the K154E substitution was found in a further 29 out of a population of 8,655 African individuals. Thus, this SNP is rare in the African population (0.003%) compared to the combined Baka/Bakola groups (20%). K154E was not found in other East or Southern African hunter-gatherer populations (such as Hadza and Sandawe) nor in the African San, who have the oldest genetic lineages among humans [30] (S4B Fig); it was also not identified in Neanderthal and Denisovan lineages (denoted as ‘archaic’ in S4B Fig). However, E154 is encoded in the IFN λ 4 orthologue for the chimpanzee, *Pan troglodytes* (Pt), our closest mammalian species. Notably, the human TT allele encodes a potential K154 codon [18] suggesting that the E154K substitution arose in humans prior to *IFNL4* pseudogenisation. Together with the fact that nearly all humans encode K154, these data suggest that the less active E154K substitution emerged early during human evolution after the divergence of our last common ancestor with chimpanzees.

Functional comparison of primate IFN λ 4 orthologues

Since a lysine residue encoded at position 154 is unique to humans compared to other mammalian species (Fig 2A) [31], we compared wt HsIFN λ 4 and its K154E variant to wt PtIFN λ 4 and an equivalent ‘humanised’ PtIFN λ 4 E154K mutant in both the EMCV and ISG induction assays as well as a CRISPR-Cas9 cell line in which the EGFP coding region had been introduced into the endogenous *ISG15* gene upstream of and in-frame with the *ISG15* open reading frame (ORF) (S5 Fig). This cell line offered advantages over other approaches since it facilitated measurement of ISG induction of an endogenous gene by assessing EGFP fluorescence across a range of dilutions of secreted IFN λ s (S5B Fig).

Although intracellular expression levels of each IFN λ 4 variant were similar, (Fig 2B), wt PtIFN λ 4 was significantly more active than HsIFN λ 4 in each assay and had approximately equivalent activity to the HsIFN λ 4 K154E variant in signalling as well as antiviral assays (Fig 2C–2E). Converting PtIFN λ 4 to encode the E154K variant significantly decreased activity to levels that were similar to those for wt HsIFN λ 4 (encoding lysine at position 154). Extending the analysis to include rhesus macaque IFN λ 4 (*Macaca mulatta*, MmIFN λ 4) gave the same pattern whereby wt MmIFN λ 4 with E154 had greater activity than its K154 variant. However, wt MmIFN λ 4 was less active than either the human or chimpanzee IFN λ 4 with E154 indicating that other genetic differences likely modified MmIFN λ 4 activity in our assays. Consistent with the hypothesis that additional genetic differences affect susceptibility to E154K, introducing a lysine into the equivalent position of HsIFN λ 3 had a much lesser effect on its activity compared to IFN λ 4 (Fig 2C–2E). Overall, we observed a similar ~100-fold enhancement of activity for E154 over K154 for each of the IFN λ 4 orthologues in anti-EMCV activity and EGFP IFN reporter induction. Thus, we conclude that wt HsIFN λ 4 has attenuated activity principally because of a single amino acid change at position 154.

Comparison of the spectrum of antiviral activity of HsIFN λ 4 E154 versus K154

To broaden analysis of the impact of a lysine residue compared to a glutamic acid at position 154 in HsIFN λ 4, antiviral assays were conducted with other human viruses that are less sensitive to exogenous IFN compared to EMCV, and on different cell lines. Specifically, we used

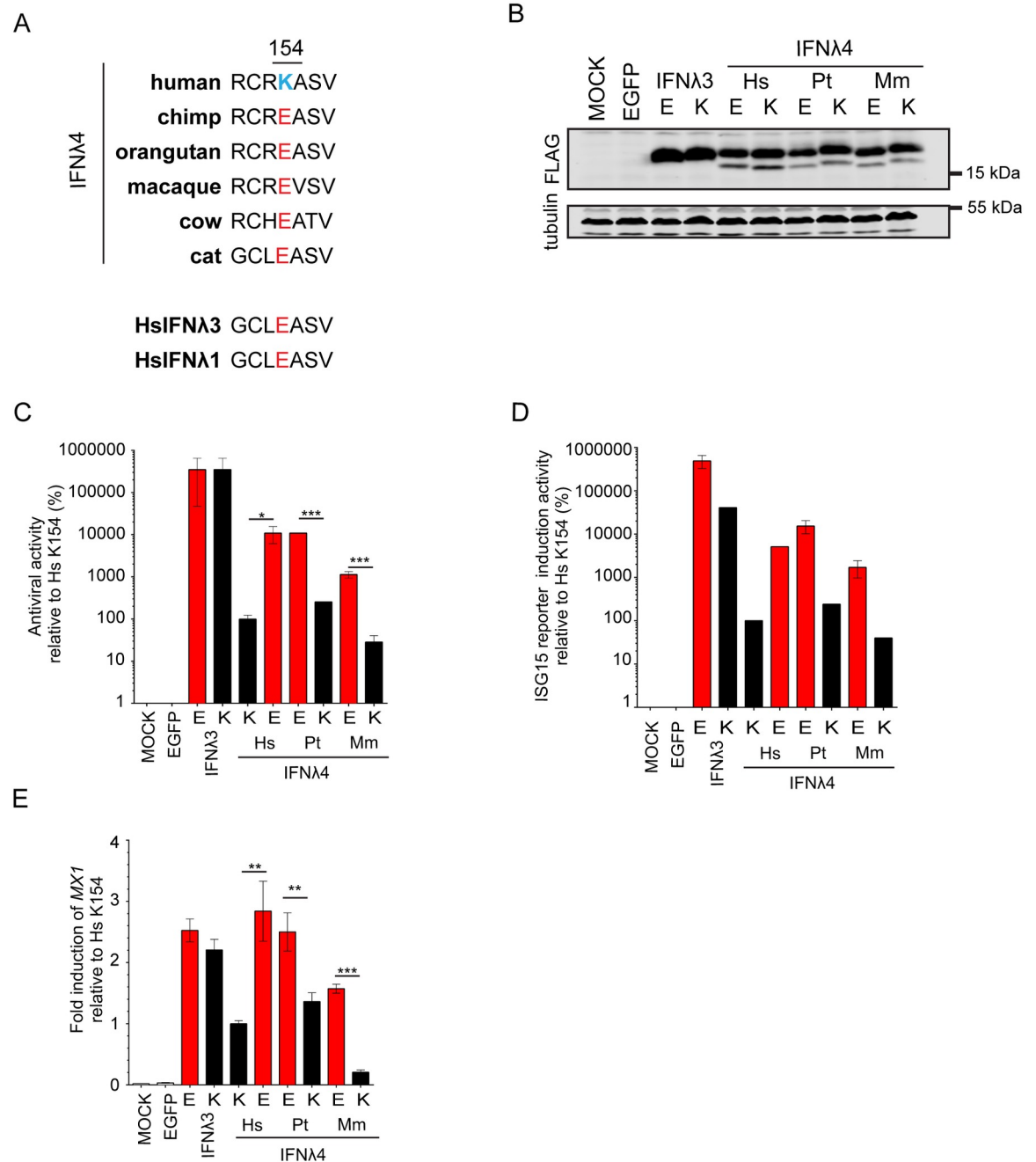


Fig 2. Human IFNλ4 is less active than chimpanzee IFNλ4 due to a substitution at amino acid position 154. (A) Amino acid alignment from positions 151 to 157 for selected orthologues of HsIFNλ4 from different species as well as 2 human paralogues (HsIFNλ1 and HsIFNλ3). At position 154, HsIFNλ4 encodes a lysine (K; blue) while sequences from all other species predict a glutamic acid at this site (E; red). (B) Western blot analysis of intracellular IFNλ4 from different species encoding E or K at position 154 as well as equivalent E and K variants of HsIFNλ3op. HEK293T cells were transfected with the relevant plasmids for 48 hrs prior to preparation of cell lysates. IFNλ4 variants were detected with anti-FLAG antibody ('FLAG') and tubulin was used as a loading control. Mock- and EGFP-transfected cells were used as negative controls. (C) EMCV antiviral assay in HepaRG cells of IFNλ from the different species indicated (human [Hs], chimpanzee [Pt] and macaque [Mm]) encoding an E (red bars) or K (black bars) at position 154 alongside the equivalent amino acid substitutions in HsIFNλ3op. Antiviral activity is shown relative to that for HsIFNλ4 in HepaRG cells. Order denotes wt then variant IFNλ for each species. Data show +/- SD of biological replicates (n = 3) and are representative of two independent experiments performed on different days. *** = <0.001; * = <0.05 by unpaired, two-tailed Student's T test comparing 154E and 154K for each IFN. (D) IFN signalling reporter assay in HepaRG.EGFP-ISG15 cells of IFNλ from the different species indicated (human [Hs], chimpanzee [Pt] and macaque [Mm]) encoding an E (red bars) or K (black bars) at position 154 alongside the equivalent amino acid substitutions in HsIFNλ3op. Activity is shown relative to that for HsIFNλ4 in HepaRG.EGFP-ISG15 cells. Order denotes wt then variant IFNλ for each

species . . . Serial two-fold dilutions of CM (1:2 to 1:2097152) were incubated with the cells for 24 hrs and EGFP-positive cells (%) were measured by flow cytometry at each dilution and the IC_{50} value was calculated. Data shown are mean \pm SEM of biological replicates ($n = 3$) and are representative of two independent experiments carried out on different days. Comparison of all E versus K substituted forms of IFN $\lambda 4$ within a homologue yielded significant values ($p = <0.001$ by Two-way ANOVA). (E) *MX1* gene expression measured by RT-qPCR for IFN $\lambda 4$ from different species encoding an E (red bars) or K (black bars) at position 154 alongside the equivalent amino acid substitutions in HsIFN $\lambda 3op$. Data represent the relative fold change of *MX1* mRNA by RT-qPCR in cells stimulated with CM (dilution 1:4) for 24 hrs compared to HsIFN $\lambda 4$ wt. Data show average \pm SEM of biological replicates ($n = 6$) combined from two independent experiments performed on different days. *** = <0.001 ; ** = <0.01 by unpaired, two-tailed Student's T test comparing 154E and 154K from each species.

<https://doi.org/10.1371/journal.ppat.1007307.g002>

HCV infection in Huh7 cells as well as infectious assays with influenza A virus (IAV) and Zika virus (ZIKV) in A549 cells against single high dilutions of each IFN. As controls, we also included the less active P70S and L79F HsIFN $\lambda 4$ variants alongside HsIFN $\lambda 3op$ in these assays. Using the HCVcc infectious system in Huh7 cells, HsIFN $\lambda 4$ K154E significantly decreased both viral RNA abundance compared to wt protein and exhibited a trend towards a lower number of infected viral antigen (NS5A)-positive cells (Fig 3A, upper and lower panels respectively). Furthermore, we performed assays examining HCV entry (HCV pseudoparticle system [HCVpp]), viral RNA translation and RNA replication (both assessed with the HCV sub-genomic replicon system). There was no significant difference in the efficiency of HCVpp infection between wt HsIFN $\lambda 4$ and any of the three variants tested in the MLV-based pseudoparticle assay (Fig 3B, upper panel). However, we did observe a greater inhibition when the non-HCV E1E2-containing PPs were used, potentially reflecting the higher efficiency or different mode of entry of HCVpp entry compared to non-glycoprotein-containing retroviral PPs that could saturate an inhibitory response (Fig 3B, lower panel). wt HsIFN $\lambda 4$ reduced HCV RNA replication compared to EGFP and introducing the K154E mutation into wt HsIFN $\lambda 4$ gave a further significant reduction in replication. (Fig 3C, upper panel). However, primary translation of input viral RNA was not affected by HsIFN λ addition (Fig 3C, lower panel). To examine further the inhibitory effect of wt HsIFN $\lambda 4$ and the K154E variant on viral RNA replication, Huh7 cells that constitutively expressed a HCV sub-genomic replicon [Tri-JFH1; 32] were treated with both forms of the protein over several passages (S6A Fig). Our results revealed a consistent decrease in HCV RNA levels over 8 passages spanning 25 days with the K154E variant exerting a greater inhibition on RNA replication compared to wt HsIFN $\lambda 4$; consistent with this conclusion, fewer sub-genomic replicon-bearing cells survived treatment with HsIFN $\lambda 4$ K154E than the wt protein (S6B and S6C Fig). Thus, HsIFN $\lambda 4$ reduces HCV RNA replication and the K154E variant exerts greater potency against this stage in the virus life cycle. HsIFN $\lambda 4$ K154E also reduced titers of IAV and ZIKV to a greater extent than wt protein in A549 cells (~10-fold; Fig 3D and 3E). Although this was only statistically significant in the context of IAV, a similar trend was evident with ZIKV for the K154E variant compared to wt HsIFN $\lambda 4$. We found that the P70S and L79F variants consistently reduced the ability of wt HsIFN $\lambda 4$ to protect against infection in most assays. Taken together, our data further confirmed the greater antiviral activity associated with converting a lysine residue at position 154 in HsIFN $\lambda 4$ to a glutamic acid residue.

Transcriptomic analysis of cells stimulated with HsIFN $\lambda 4$ variants

The enhanced antiviral activity of HsIFN $\lambda 4$ E154 against multiple viruses in different cell lines suggested that this variant may differentially affect global transcription of antiviral ISGs. To test this hypothesis and examine the impact of HsIFN $\lambda 4$ on global transcription, A549 cells were treated with wt and variant forms of HsIFN $\lambda 4$ that had different antiviral activities and transcriptional changes were analysed by RNA-Seq at 24 hrs post stimulation (Fig 4). A549

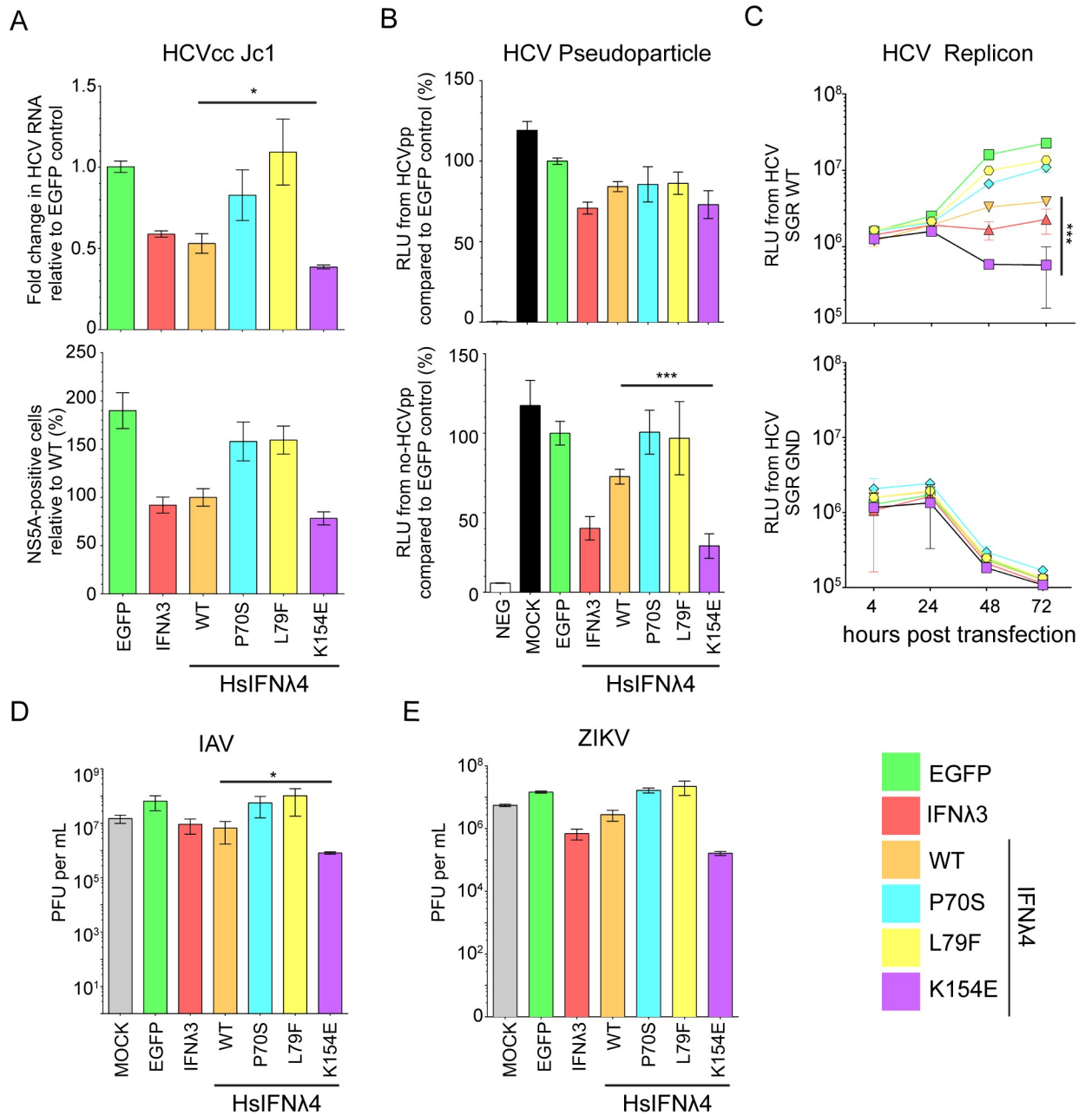


Fig 3. HsIFNλ4 E154 has greater antiviral activity compared to wt HsIFNλ4 K154. (A) Antiviral activity of HsIFNλ4 variants against HCVcc infection in Huh7 cells measured by RT-qPCR of viral RNA (upper panel) and virus antigen-positive cells (HCV NS5A protein; lower panel). HsIFNλ-containing CM (1:3) was incubated with Huh7 cells for 24 hrs before infection with HCVcc Jc1 (MOI = 0.01). HCV RNA was measured by RT-qPCR on RNA isolated at 72 hpi. Results shown are relative to infection in cells treated with EGFP CM (upper panel) or wt HsIFNλ4 (lower panel). Data show +/- SEM (n = 6) combined from two independent experiments performed on different days. * = <0.05 by unpaired, two-tailed Student's T test comparing wt and K154E. (B) The effect of HsIFNλ4 variants on JFH1 HCV pseudoparticle (pp) infectivity in Huh7 cells. Relative light units (RLU) in the lysate of luciferase-expressing MLV pseudoparticles following inoculation of Huh7 cells stimulated with CM (1:3), relative (%) to CM from EGFP-transfected cells. The upper panel shows data from MLV pseudoparticles containing JFH1 glycoproteins E1 and E2 while the lower panel indicates data from MLV pseudoparticles that lack E1 and E2 (MLV core particles). Luciferase activity was measured at 72 hrs after inoculation. Error bars show +/- SEM of biological replicates (n = 6). (C) The effect of HsIFNλ4 variants on transient HCV RNA replication (upper panel) and translation (lower panel) using a subgenomic replicon assay in Huh7 cells. Huh7 cells were treated with CM (1:3) for 24 hrs before transfection with *in vitro* transcribed JFH1 HCV-SGR RNA expressing *Gaussia* luciferase; the upper and lower panels show data from wt (replication competent) and GND (non-replicative) sub-genomic replicons respectively. RLU secreted into the media was measured at 4, 24, 48 and 72 hpt. Error bars show +/- SD of biological replicates (n = 3). Data are representative of two independent experiments performed on different days. *** = <0.001 by two-way ANOVA on wt versus K154E. Comparing wt and K154E RLU at 72h by two-tailed

Student's T-test gave a significant difference $** = <0.01$. Antiviral activity of wt and variant HsIFN λ 4 on IAV (WSN strain) (D) or ZIKV (strain PE243). (E) infection in A549 cells as determined by plaque assay of virus released from infected cells at 48 hpi for IAV or 72 hpi for ZIKV. HsIFN λ 4-, HsIFN λ 3- and EGFP-containing CM (1:3) was incubated with A549 cells for 24 hrs before infection with IAV strain (MOI = 0.01 PFU/cell). Supernatant was harvested and titrated on MDCK cells for IAV or Vero cells for ZIKV. Error bars show +/- SEM of biological replicates (n = 3). * = <0.05 by unpaired, two-tailed Student's T test comparing wt and K154E.

<https://doi.org/10.1371/journal.ppat.1007307.g003>

cells were used because they recapitulate the functional differences in HsIFN λ s as observed in other cell types and are widely used as a cell line model for epithelial antiviral immunity. The data revealed that K154E induced the broadest profile of significantly differentially-regulated genes (n = 273) compared with either the wt protein (n = 178) or the P70S variant (n = 115; [Fig 4A–4C and S2 Data](#)). The pattern of genes induced by the positive control HsIFN λ 3op and HsIFN λ 4 K154E were very similar ([Fig 4B and 4C](#)). From IPA pathway analysis, all HsIFN λ s induced the same transcriptional programmes with differences in the overall significance of these pathways, most notably enhancement of the antigen presentation and protein ubiquitination pathways with the K154E variant ([Fig 4D](#)). Many of the differentially-expressed genes shared by HsIFN λ 4 wt, K154E and P70S included known restriction factors with antiviral activity (e.g. *IFI27*, *MX1*, *ISG15*; [Fig 4E](#)) although the magnitude of induction was consistently greatest for HsIFN λ 4 K154E ([Fig 4F](#)). There were also several ISGs that only achieved significant induction by K154E and HsIFN λ 3op (e.g. *IDO1*, *IRF1* and *ISG20*; [Fig 4E and 4F](#)). We predict that the apparent selectivity by IFN λ 4 K154E results from the greater potency of this variant compared to wt. HsIFN λ 4 and the P70S variant allowing genes to reach the significance threshold ([Fig 4F](#)). Enhanced production of antiviral genes in cells treated with HsIFN λ 4 E154 would explain differences in antiviral activity against EMCV, HCV, IAV and ZIKV.

Comparison of human and chimpanzee intrahepatic gene expression during HCV infection

Direct *in vivo* validation of our transcriptomic findings alone on the enhanced activity of the K154E variant would require liver biopsy samples from either HCV-infected Pygmies or chimpanzees combined with equivalent samples from infected humans encoding wt HsIFN λ 4. This was not possible since such tissue samples are not available from the Pygmy population infected with HCV and biopsies from acutely infected individuals are exceptionally rare. Moreover, chimpanzees are no longer used for experimental studies for ethical reasons. Therefore, we compared lists of reported differentially-expressed genes during acute HCV infection in humans and chimpanzees from the available literature. In the case of humans, there is only one report that analyses the transcriptional response in acute infection [33]. For chimpanzees, gene expression analysis is available from four independent studies [34–37] which include longitudinal data from serial biopsies. Therefore, all of the data was collated and we focused our comparisons on periods when human and chimpanzee biopsies were taken across the same time period after initial HCV infection (between 8 and 20 weeks post infection).

Comparative gene expression analysis revealed distinct host responses in humans and chimpanzees as well as overlapping differentially-regulated genes ([Fig 5A and S3 Data](#)). In chimpanzees, the transcriptional profile contained significantly expressed genes that were type I/III IFN-regulated ISGs known to restrict HCV infection (*RSAD2*, *IFI27* and *IFIT1*) [2], as well as genes involved in antigen presentation and adaptive immunity (*HLA-DMA* and *PSMA6*). These genes were not significantly differentially expressed in humans, whose response was mainly directed towards up-regulation of pro-inflammatory genes (for example, *CXCL10*, *CCL18* and *CCL5*) and metabolism genes (*AKR1B10* and *HKDC1*) ([Fig 5A and S3](#)

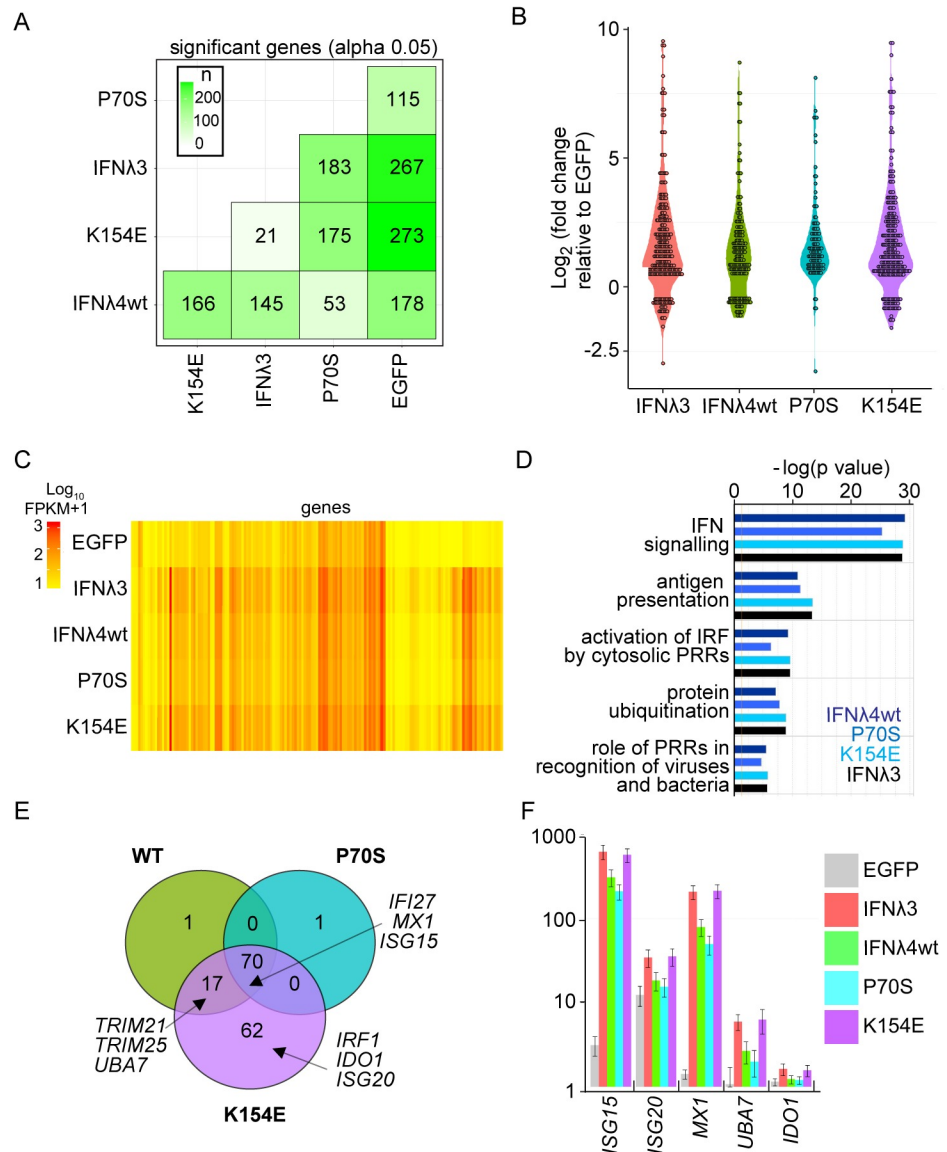


Fig 4. HsIFNλ4 E154 induces more robust antiviral gene expression than the wt K154 variant. A549 cells were treated with CM (1:3 dilution) for 24 hours from cells transfected with plasmids expressing the different HsIFNλs and EGFP. After isolation of RNA, transcriptome analysis was carried out by RNA-Seq. (A) Total number of significantly differentially-expressed genes in each experimental condition (x-axis) relative to each other condition (y-axis). Colour shaded by differences in numbers of transcripts between sample 1 (x-axis) and sample 2 (y-axis) are shown. (B) Violin plot of all significant, differentially-expressed genes (over two-fold) (log₂ fold change for each condition compared to RNA from cells treated with EGFP). CM was obtained from cells transfected with HsIFNλ3op (red); HsIFNλ4 wt (green); HsIFNλ4 P70S (cyan), and HsIFNλ4 K154E (purple). (C) Heat map of all significantly differentially-expressed genes (over two-fold) (log₁₀ Fragments Per Kilobase of transcript per Million mapped reads (FKPM) in each experimental condition including EGFP CM-stimulated cells. Genes shown as columns and values are not normalised to negative control. (D) Pathway analysis using IPA on all significantly differentially-expressed genes (>2 fold) for each variant compared to EGFP. The top five most significantly induced pathways are shown [-log(p value)]. (E) Comparison of differentially-expressed genes (significant and at least 2-fold difference) stimulated by the HsIFNλ4 variants (HsIFNλ4 wt in green, HsIFNλ4 P70S in cyan and HsIFNλ4 K154E in purple) illustrated by a Venn diagram showing shared and unique genes. Three examples in overlapping and unique areas of the Venn diagram are highlighted. (F) Raw gene expression values (FKPM+1) for representative genes from core, shared and K154E-'specific' groups for the different treatments. Data are shown as mean +/- SD of biological replicates (n = 3). Exemplary genes selected were: *ISG15* and *MX1* (core), *UBA7* (not significantly induced by P70S), and *ISG20* and *IDO1* (apparently specific for K154E). All transcriptomic analysis and gene lists are available in [S2 Data](#).

<https://doi.org/10.1371/journal.ppat.1007307.g004>

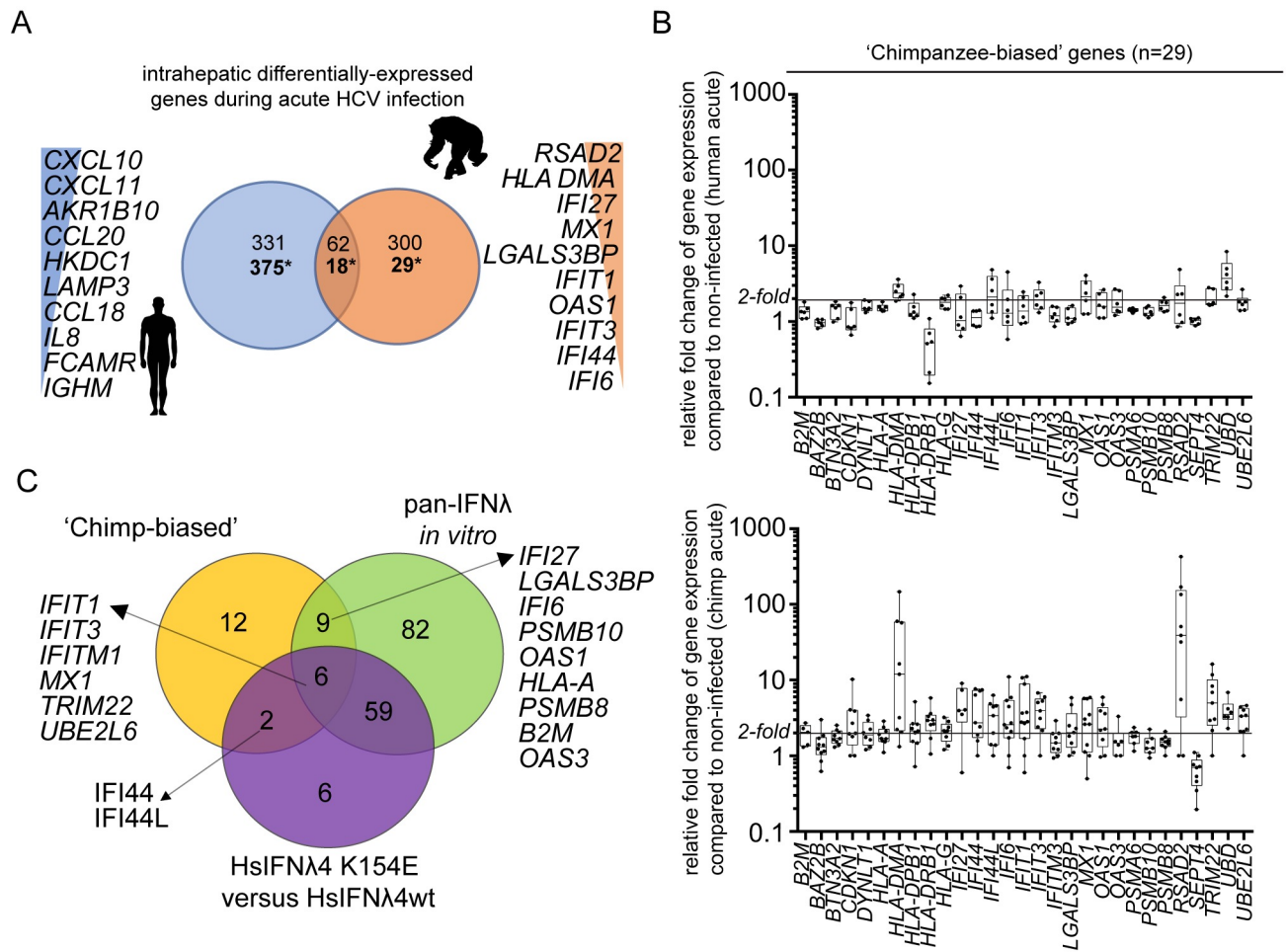


Fig 5. Chimpanzees induce greater levels of antiviral ISG expression during HCV infection *in vivo*. (A) Numbers of shared and unique differentially-expressed genes in liver biopsies from HCV-infected humans (blue) and experimentally-infected chimpanzees (orange) during the acute phase of infection represented as a Venn diagram (also see [S1 Data](#)). Gene expression during a time period of between 8 and 20 weeks was used where comparable published data for both species exists. The top ten species-'specific', differentially-expressed genes are shown ranked by levels of expression. Two sets of values for each comparison are shown; above shows the total differentially-expressed genes from at least one study while * highlights the value relating to the 'core' chimpanzee analysis that considered only the genes differentially-expressed in at least two studies of chimpanzee acute HCV infection. (B) Fold change of expression compared to controls (two uninfected individuals) for the 29 'chimpanzee-biased' genes in humans (upper) and chimpanzees (lower) shown as box plot and whiskers. Data are shown as box and whiskers to indicate median and range. Each value is illustrated by a black circle. The chimpanzee values represent an average of all fold changes for each chimpanzee over the time period. (C) Venn diagram analysis comparing the 29 chimpanzee-biased genes to the RNA-Seq data for all IFNs (GFP versus IFN) and for HsIFNλ4 K154E versus wt specifically. Illustrative gene names are shown as examples. All data are available in [S2 Data](#).

<https://doi.org/10.1371/journal.ppat.1007307.g005>

Data). This was consistent with previous characterisation of the human acute response to HCV infection that failed to detect a major type I/III IFN signature but predominantly found a type II or IFN-gamma-mediated response [33]. From the available longitudinal data, the 'chimpanzee-biased' differentially-expressed genes were induced early in infection and remained significantly up-regulated during the acute phase following an early peak after infection ([S7A and S7B Fig](#)). Differences were also reflected in pathway analysis in terms of the most significant pathways and their overall levels of significance ([S3 Data](#)). For example, the 'chemokine-mediated signalling pathway' was upregulated in humans but not chimpanzees whereas the T cell receptor signalling pathway which was modulated in chimpanzees was not significantly altered in humans. Inspection of the raw data from humans indicated that many

apparently ‘chimpanzee-biased genes’ were expressed but did not reach significance in the original study. These genes were typically induced at a lower level in the human group when compared to averaged values for chimpanzee studies across the similar time period (Fig 5B). Furthermore, there was a greater induction of antiviral ISGs in chimpanzees during chronic infection in comparison to humans although to a less pronounced effect (S7C Fig).

From examining the *in vivo* biopsy data, we identified a group of 29 chimpanzee-biased genes in liver biopsies that were seemingly up-regulated during acute infection to a greater extent compared to humans. Comparing this set of genes to those from the RNA-Seq transcriptomic data obtained *in vitro* (Fig 4) showed that the majority (17/29 genes) of the chimpanzee-biased genes were induced by HsIFN λ 4 stimulation, with approximately half (8 genes) of those being significantly up-regulated to a great extent with K154E compared to wt, including *MX1*, *IFITM1*, *IFIT1*, *IFIT3*, *TRIM22* and *IFI44L* (Fig 5C). Thus, there are similarities between our *in vitro* analysis and published *in vivo* studies that would correlate with differences in IFN λ 4 activity between humans and chimpanzees.

Mechanism of action for the enhanced activity of the HsIFN λ 4 E154 variant

Having established the greater antiviral potential for the E154 IFN λ 4 variant and its apparent evolutionary relevance, we set out to determine the possible basis for its enhanced activity. No crystal structure for HsIFN λ 4 is available but a homology model based on comparison with the IFN λ 3 structure has been reported [24]. We expanded this predicted model based on both of the IFN λ 1 and IFN λ 3 crystal structures to explore the possible impact of K154E, P70S and L79F on IFN λ 4 function (Fig 6A and S8 Fig; [38,39]). As has been previously described, the sequences in helix F, which binds to IFN λ R1, are relatively well conserved [18,24]. The position equivalent to amino acid 154 in IFN λ 4 is a glutamic acid in both IFN λ 1 and IFN λ 3 (amino acid position 176 in IFN λ 1 and 171 in IFN λ 3) and its side chain faces inward towards the opposing IL10R2-binding helices C and D (Fig 6A). The free carboxyl group of glutamic acid forms non-covalent intramolecular interactions with two non-linear segments on IFN λ 1 and 3 (IFN λ 1 residue K64, and in IFN λ 3 K67 and T108). In IFN λ 4, these E154-interacting positions are not conserved compared to IFN λ 1/3 although homologous positions do exist with biochemically similar residues (IFN λ 4 R60, and R98 that lies just upstream of the residue homologous to IFN λ 3 T108).

To test whether the biochemical properties of glutamic acid at position 154 contribute to IFN λ 4 activity, a panel of variants was constructed with biochemically distinct amino acids (R154, L154, A154, D154 and Q154). Firstly, intracellular expression of each variant at position 154 was approximately equivalent (Fig 6B). In signalling assays, the order of activity was E>Q/D>A>L>K>R (S9A Fig). We found a similar pattern in the EMCV antiviral assays except that L154 had the least activity (Fig 6C). We interpret these findings to conclude that E154 is biochemically the most favoured residue at this position with regards to antiviral potential, and that substitution of E154 to lysine results in the lowest potency for IFN λ 4 activity. Interestingly, both Q154 and D154 had ‘intermediate’ activity compared to E154 and K154, suggesting that side chain length and negative charge are important to maximise the activity of IFN λ 4.

In a final series of experiments aimed at giving further insight into the mechanism of action of IFN λ 4 K154E, we compared the relative activities and abundance of different IFN λ 4 variants in cell lysates (i.e. intracellular protein) and supernatants (i.e. extracellular protein). As wt HsIFN λ 4 is poorly secreted into the supernatant from transfected cells in the absence of enrichment [24,40], IFN λ 4 in CM was immunoprecipitated using an anti-FLAG antibody. In

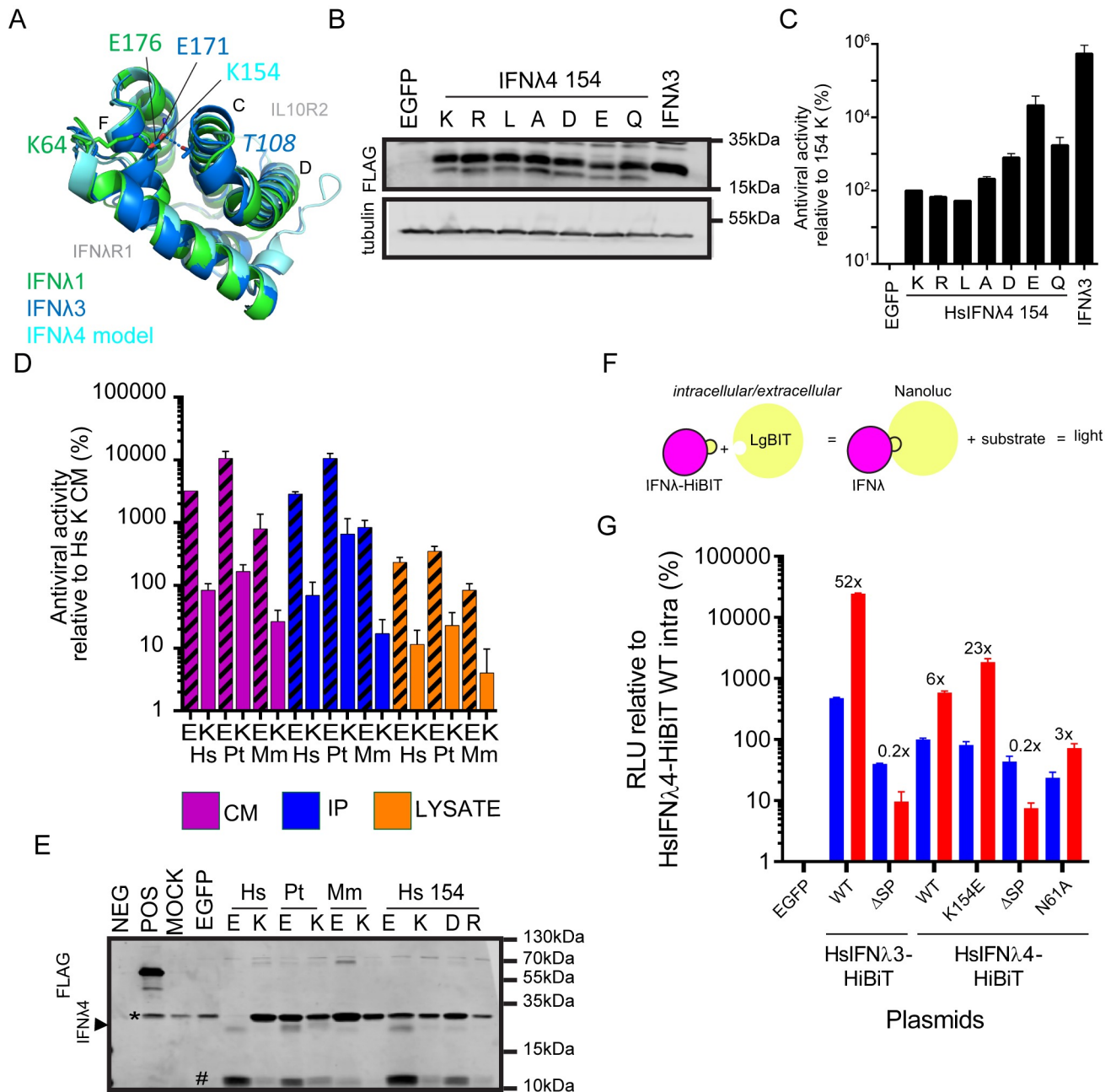


Fig 6. Mechanism of action of the IFNλ4 K154E variant. (A) Modelled structure of HsIFNλ4 showing position 154 at a central location in the molecule with reference to receptor subunit-binding interfaces (IFNλR1 and IL10R2). Overlapping crystal structures for HsIFNλ1 (green) and HsIFNλ3 (dark blue) are overlaid together with a homology model for HsIFNλ4 (light blue). In the overlapping structures, the homologous positions for HsIFNλ4 E154 (E176, IFNλ1; E171, IFNλ3) make intramolecular non-covalent interactions with two distinct regions within IFNλ. (B) Detection of intracellular IFNλ4 154 mutants (K, R, L, A, D, E and Q) by Western blot analysis of lysates from plasmid-transfected producer HEK293T cells. The IFNλ4 variants were detected with an anti-FLAG antibody. Tubulin was used as a loading control. (C) Antiviral activity of HsIFNλ4 IFNλ4 154 mutants (K, R, L, A, D, E and Q) in an anti-EMCV CPE assay relative to CM from wt HsIFNλ4 (K154 variant) in HepaRG cells. Data show mean +/- SEM combined from three independent experiments performed on different days. (D) Antiviral activity of IFNλ4 found in CM, intracellular lysate and immunoprecipitated CM from the different species indicated (human [Hs], chimpanzee [Pt] and macaque [Mm]) encoding an E or K at position 154 in an anti-EMCV CPE assay relative to CM from wt HsIFNλ4 in HepaRG cells. Data show mean +/- SEM from two independent experiments performed on different days. (E) Detection of extracellular IFNλ4 from different species as well as select mutants at position 154 (E, K, D and R) by Western blot analysis of samples of FLAG-tag immunoprecipitated CM (1 ml) from plasmid-transfected producer HEK293T cells. A BAP-FLAG fusion protein was used as an immunoprecipitation control (POS). The IFNλ4 variants were detected with an anti-FLAG antibody. A FLAG-positive lower molecular weight product, which is potentially a degradation product is highlighted with a #. An upper band running near to the IFN is shown (*) which is likely antibody fragments from the immunoprecipitation reaction. Blot is representative of three independent experiments. (F) Schematic of the split NanoLuc Luciferase assay to measure

the relative abundance of intra- and extracellular abundance of HsIFN λ 3 and HsIFN λ 4 variants produced in plasmid-transfected cells. (G) Levels of luciferase activity (RLU) relative to intracellular enzyme activity in cells expressing wt IFN λ 4 (set at 100%). Intra- and extracellular luciferase activities are shown in blue and red respectively. The constructs used are indicated below the graph. The ratio of intra- to extracellular RLU values are indicated for each construct.

<https://doi.org/10.1371/journal.ppat.1007307.g006>

antiviral assays, the activity of human, chimpanzee and macaque E154 variants from cell supernatants, IP fractions and lysates was greater than the corresponding K154 variants in agreement with our earlier results (**Fig 6D** and **Fig 2C–2E**). Moreover, the D154 and R154 variants yielded patterns for cell lysates, cell supernatants and immunoprecipitated IFN λ 4 protein such that D154 had intermediate activity between E154 and K154 while R154 had approximately equivalent activity to K154 (**S9B Fig**). Thus, each variant displayed a similar pattern of activity irrespective of the source of IFN λ 4. From Western blot analysis, the E154 and K154 variants for each individual species were detected at similar levels in cell lysates (**S9C Fig**). The HsIFN λ 4 D154 and R154 variants were expressed to slightly higher and lower levels respectively compared to E154 and K154 from humans. Paradoxically, we did not find the same pattern in IFN λ 4 abundance for immunoprecipitated protein derived from cell supernatants. Thus, we were able to detect greater amounts of the E154 variants for human, chimpanzee and macaque IFN λ 4 compared to their K154 variants (**Fig 6E** and **S9D Fig**). It was not possible to reliably detect macaque K154 or human R154 variants. HsIFN λ 4 D154 had levels intermediate between the E154 and K154 variants. By Western blot and subsequent densitometry analysis, the relative abundance of IFN λ 4 E154 and K154 variants in cell lysates for any species differed by 1.3 fold yet the approximate fold increase in antiviral activities were significantly greater and on average 16-fold. For the secreted IFN λ 4 variants, we found that not only was there a higher abundance of E154 to K154 protein (9-fold), but activity was 41-fold higher for E154 than K154 variants, which results in a significant 3 to 4-fold rise in antiviral activity not explained by protein abundance (**S9E Fig**). With the exception of macaque K154, the FLAG antibody detected a putative breakdown product of about 11kDa in each of the samples, which we presume arose from cleavage by an unknown intracellular protease as it was also detected in cell lysates. The amount of this lower molecular weight product followed the same pattern as the full-length protein in that there was more with E154 than K154 thus cleavage does not explain differences in antiviral activity.

Towards the end of the study, the split NanoLuc reporter system became available [41], which comprised an 11 amino acid HiBiT tag that could replace the FLAG tag at the C-terminal end of the HsIFN λ 4 variants and reconstitute luciferase activity (**Fig 6F**). The advantage of this approach was that the relative secretion of each variant could be determined by comparing enzyme activity from cell lysates and culture media in a highly-quantitative manner. Moreover, the antiviral activity of HiBiT-tagged HsIFN λ 4 variants could be compared to their respective FLAG-tagged versions. To demonstrate the capacity of the system to quantify secretion, we generated HiBiT-tagged versions of wt HsIFN λ 3 and HsIFN λ 4 with and without N-terminal signal sequences, which would abrogate secretion. Removing the signal sequences from either HsIFN λ protein reduced secretion by fivefold (**Fig 6F** and **6G**). The non-natural N61A variant that is not glycosylated was secreted ~2-fold less efficiently than wt HsIFN λ 4. In agreement with our data using FLAG-tagged HsIFN λ 4, the K154E variant of HsIFN λ 4 was secreted about 3 times more efficiently than the wt protein (**Fig 6F** and **6G**). In a subsequent screen of all HsIFN λ 4 natural variants with the HiBiT tag system, we also validated the data shown in **Fig 1C** and **S2 Fig (S10A–S10C Fig)**. Moreover, HiBiT-tagged HsIFN λ 4 K154E was >10-fold more active than the wt form (**S11C Fig**). Thus, both FLAG- and HiBiT-tagged

forms of K154E gave higher antiviral activity and were secreted more efficiently than wt HsIFN λ 4.

Lastly, to examine secretion in more detail, cells that had been transfected with HiBiT-tagged HsIFN λ 3 and HsIFN λ 4 variants were treated with Brefeldin A (BFA) and Monensin to block ER and Golgi transport respectively (S11A–S11C Fig). Treatment with these inhibitors disrupted secretion of HsIFN λ 3 by 12- (BFA) and 25-fold (Monensin). For the HsIFN λ 4 K154E variant, each of the inhibitors blocked secretion by about 10–12-fold. In the case of wt HsIFN λ 4, BFA inhibited secretion to a greater extent (~20-fold) than for either HsIFN λ 3 or HsIFN λ 4 K154E whereas Monensin decreased secretion to a similar extent for all three proteins. The explanation for the slightly greater inhibition of HsIFN λ 4 by BFA requires further investigation. Overall, our data conclusively demonstrate that glutamic acid at position 154 promotes greater antiviral potential by enhancing both IFN λ 4 secretion from cells and its intrinsic potency.

Discussion

In this study we have identified further functional variants of human and non-human IFN λ 4 that expand the spectrum of its activity. By comparing IFN λ 4 from different species we demonstrate that the genus *Homo* evolved an IFN λ 4 gene with attenuated activity (prior to the TT allele), and that the vast majority of extant humans carry an IFN λ 4 variant with lower antiviral potential due to a mutation of a single highly-conserved amino acid residue (E154K). Human African hunter-gatherer Pygmies and chimpanzees encode a more active IFN λ 4 (E154). We speculate that position 154 in IFN λ 4 plays a key role in intramolecular interactions that may facilitate stabilisation of the protein thereby influencing its secretability and antiviral activity (S12 Fig).

Implications of the E154K substitution for IFN λ 4 evolution

Our analysis suggests that the *Homo* IFN λ 4 orthologue acquired the E154K substitution, yielding a less active protein, after the genetic divergence of the hominid *Homo* and *Pan* ancestral lineages (estimated to be at most 6 million years ago in Africa [42]) but before human/Neanderthal divergence (~370,000 years ago, [43]). Subsequently, the *IFNL4* gene acquired two further variants, the P70S and TT alleles that are now common in the human population [18]. Acquisition of each of these alleles either further reduced (P70S) or abolished (TT) IFN λ 4 activity. Other rare variants have arisen in humans with little impact on HsIFN λ 4 antiviral potential based on our *in vitro* assays, except for variants L79F and K154E, which lower and increase activity respectively. To us, the most intriguing of these variants is K154E, which was found in a high proportion of rainforest ‘Pygmy’ hunter-gatherers from west central Africa [28] but was rarely present in the African population. Since this variant was not present in the genetic data for San and Archaic Neanderthal and Denisovan human lineages, we speculate that these populations likely reacquired K154E following divergence of chimpanzees and humans. However, with the ever-increasing availability of genetic data from ancient and extant human populations, it may be possible to identify other populations carrying the E154 variant; in particular more details on the demographics of the 29 African individuals in the gnomAD database [29] may address whether there are additional specific groups who carry this more active variant and how it arose.

The factors responsible for divergent functional evolution of the *IFNL4* gene within and between species are not known. It has been demonstrated that loss of *IFNL4* has evolved under positive selection in some human populations thus we speculate that differences in exposure to certain pathogenic microbes has driven evolution of the E154 variant. On the one hand, type

III IFN signalling enhances disease and impedes bacterial clearance in mouse models of bacterial pneumonia [44]. This suggests that IFN λ 4 with a lower activity could be beneficial during non-viral infections although a link between *IFNL4* genotype and bacterial infection in humans has not yet been made. Conversely, we postulate that the presence of more active IFN λ 4 exemplified by E154 in Pygmies and chimpanzees may be linked to increased exposure to zoonotic viral infections in the Congo rainforest, such as pathogenic Filovirus infections [45].

The impact of IFN λ 4 functional differences on virus infection

For decades, experimental studies in chimpanzees have provided unique insight into HCV infection [46] but they do not present with identical clinical outcomes as human subjects. For example, chimpanzees have been reported to clear HCV infection more efficiently than humans [47], rarely develop hepatic diseases similar to humans [48], and are refractory to IFN α therapy [49]. Moreover, HCV evolves more slowly in infected chimpanzees, possibly due to a stronger immune pressure that reduces replication compared to humans [50]. In humans, *IFNL4* genetic variants are associated with, and thought to regulate, each of these characteristics [18,51,52]. Although myriad factors could explain these phenotypic differences, including differences in antagonism of the immune response by HCV or changes in *IFNL* transcription for example, we propose that the greater antiviral activity of PtIFN λ 4 compared to HsIFN λ 4 contributes to the distinct responses to HCV infection in the two species.

Acute HCV infection in human cells *in vitro* and chimpanzees *in vivo* selectively stimulates type III over type I IFNs, which are effective at signalling in hepatocytes [53,54]. Notably, there is no apparent type I/III IFN gene expression signature in liver biopsies from humans with acute HCV infection [33]. Differences in IFN signalling during HCV infection have been postulated to explain the ability to control HCV infection in cell culture or following IFN-based therapy in humans [55,56]. Our comparative meta-analysis of the available literature revealed an apparent enhanced expression of ISGs with anti-HCV activity as well as genes involved in antigen presentation and T cell mediated immunity in chimpanzees compared to humans. Our analysis cannot be considered conclusive given the disparate nature of the retrospective studies used in our comparisons and therefore, there are a number of caveats (e.g. the expression levels of the *IFNL* genes; the relative expression of receptors in the two species). Nonetheless, we speculate that enhanced expression of ISGs in chimpanzee liver due to higher IFN λ 4 activity could lead to greater control of viral infection by both inducing antiviral genes and by coordinating a more effective adaptive T cell response, which is critical for clearance and pathogenesis during HCV infection [57].

Based on the above speculation, we would predict that the response to HCV infection in chimpanzees may be similar in Pygmies with the K154E variant. A recent study in Pygmies from Cameroon, including the Baka and Bakola groups, showed low seroprevalence of 0.6% and no evidence of chronic HCV infection [58]. Interestingly, infection in non-Pygmy groups in Cameroon has a seroprevalence of ~17% [59]. One explanation for this difference could be higher IFN λ 4 activity in populations with the K154E variant, which may enhance HCV clearance.

How might IFN λ 4 E154K reduce antiviral activity?

In our study of three primate orthologues, glutamic acid at position 154 in IFN λ 4 provided greater antiviral activity and enhanced its ability to induce antiviral gene expression. A functional comparison of human and chimpanzee IFN λ 4 orthologues has been explored previously but no significant differences in signalling activity were observed [31]. There are substantial

differences in the methodologies used in our study and that of Paquin *et al.*, which could explain our ability to detect divergent activity, for example the size of the tag attached to IFN λ 4 and dose of protein used in assays.

Our observed functional differences between E154 and K154 did not correlate with levels of intracellular accumulation or glycosylation. However, we did find that the more active E154 variants for human, chimpanzee and macaque IFN λ 4 were detected at higher levels in the immunoprecipitated fractions from cell supernatant (CM) compared to the K154 variants; the D154 and R154 variants also were detected at a lower level than E154. Interestingly, endogenous, wt HsIFN λ 4 with K154 is not secreted to detectable levels compared to wt HsIFN λ 3 [24,40,60]. Detection of low levels of secreted wt HsIFN λ 4 by Western blot analysis requires exogenous expression of the protein and precipitation of material in the cell supernatant. Poor release of HsIFN λ 4 was not due to differences in the signal peptide of HsIFN λ 4 or HsIFN λ 3 but secretion could be ablated if the single N-linked glycosylation site was mutated [24]. Our data indicate that position 154 regulates release of intracellular IFN λ 4. Moreover, IFN λ 4s with E154 are more potent than those with K154 when correcting for the difference in amounts of protein. This increase in potency for E154 was detected in both IP protein and lysates as well as HsIFN λ 4 with different C-terminal tags. Moreover, we observed that the difference between E and K is greater in the cell released fraction than the cell lysate. The reason for this discrepancy could be explained by a number of factors that are outside of the scope of this study. Based on our modelling of the IFN λ 4 structure and further mutational analysis, glutamic acid is apparently the optimal residue at position 154.

At the biochemical level, glutamic acid has the capacity to form electrostatic bonds with charged residues in the IFN λ 4 protein and moreover it possesses a side chain which could contribute greater flexibility for such interactions. Notably, replacing glutamic acid with either aspartic acid or glutamine gave higher IFN λ 4 activity than either non-polar or positively-charged residues. These potential E154-mediated interactions occur in the region of the protein devoid of cysteine-bonds likely making the interaction between helix F (IFN λ R1-binding) and the loop connecting helices C and D (IL-10-R2-binding) particularly flexible. The putative greater structural stability facilitated by E154 may inherently increase the structural integrity of IFN λ 4 making this variant more competent for secretion and more potent in signalling through the IFN λ R1-IL10R2 surface receptor complex. Increased binding to IFN receptor complexes has been shown to enhance signalling by type I IFNs [61,62]. Further biophysical studies using highly-purified recombinant protein measuring affinity and avidity of HsIFN λ 4 wt and K154E for each receptor molecule [as in 27,39] combined with studies on the mechanism of IFN λ 4 release will help address these hypotheses.

To conclude, our study further supports a significant and non-redundant role for IFN λ 4 in controlling the host response to viral infections yet one whose activity has been repeatedly attenuated during human evolution, commencing with E154K. Taken together, this provides the foundation for more detailed investigation into the mechanism of action of IFN λ 4 and its overall contribution to host immunity in regulating pathogen infection.

Materials and methods

IFNL gene sequence analysis

All available human *IFNL4* genetic variation along with associated frequency and ethnicity data for the human population were collected from the 1000 Genomes Database available at the time of study (June 2016) [23] (<http://browser.1000genomes.org/index.html>). The reference sequence for the human genome contains the frameshift "TT" allele and so potential effects of variants on the HsIFN λ 4 predicted amino acid sequence were identified manually

following correction for the frameshift mutation (TT to Δ G). The effect of all single nucleotide polymorphisms (SNPs) on the open reading frame (ORF) was thus assessed and re-annotated as synonymous or non-synonymous changes resulting in the selection of coding variants reported here. Inspection of whole genome sequence data from African hunter-gatherers was carried out using previously published datasets [28]. We remapped the raw reads of six San individuals (four Ju|'hoan and two \ddot{K} homani San) in the Simons Genomic Diversity Project [30] to the human reference genome (hg19) and conducted variant calling using the haplotype caller module in GATK (v3). Two Ju|'hoan individuals were heterozygous at rs368234815 (TT/ Δ G genotype, **S2 Data**). The genotypes of rs368234815 in Neanderthal and Denisovan were extracted from VCF files that were downloaded from http://cdna.eva.mpg.de/denisova/VCF/hg19_1000g/ and <http://cdna.eva.mpg.de/neandertal/altai/AltaiNeandertal/VCF/>. Neanderthal and Denisovan genetic data contained only Δ G alleles (**S2 Data**). Independent validation of the SNP variant that gives rise to the K154E substitution in HsIFN λ 4 was obtained from gnomAD (http://grch37.ensembl.org/Homo_sapiens/Variation/Population?db=core;r=19:39737353-39738353;v=rs377155886;vdb=variation;vf=58909380 and https://www.ncbi.nlm.nih.gov/projects/SNP/snp_ref.cgi?rs=rs377155886). Amino acid sequences for mammalian IFN λ genes were obtained from NCBI following protein BLAST of the wt HsIFN λ 4 polypeptide sequence. Multiple alignments of IFN λ amino acid sequences were performed by MUSCLE using MEGA7. Accession numbers of specific IFN λ s used in the experimental section of this study were as follows: HsIFN λ 1: Q8IU54; HsIFN λ 3, Q8IZI9.2; and for IFN λ 4: *Homo sapiens* AFQ38559.1; *Pan troglodytes* AFY99109.1; *Macaca mullata* XP_014979310.1; *Pongo abelii* (orangutan) XP_009230852.1, *Bos taurus* (cow) XP_005219183.1, *Felis catus* (cat) XP_011288250.1.

To validate the L79F variant, genomic DNA isolated from Epstein-Barr virus-immortalised B-cell lymphoblastoid cell lines from individuals (HG03095 and NA19658) identified through the 1000 Genomes Project and International HAPMAP project as probands with the L79F substitution (rs564293856 G>A SNP) were obtained from the Coriell Institute for Medical Research. PCR was used to generate an amplicon of ~300 base pairs corresponding to the region that includes rs564293856; amplicons were column-purified (Qiagen PCR-Clean Up kit, Qiagen). Internal forward and reverse primers within the amplicon were employed to determine the sequence of the region across SNP rs564293856 by Sanger sequencing (**S13A and S13B Fig**). The resulting chromatograms were inspected manually and the sequences at rs564293856 were called when identified using primers from both directions. HG03095 was confirmed as heterozygous for rs564293856 as predicted although we failed to detect the variant in NA19658; HG03095 and NA19658 were individuals who originated from Africa and America respectively.

Structural modelling

The homology model of the HsIFN λ 4 structure used in **Fig 6 and S8 Fig** was generated using the RaptorX online server (<http://raptorx.uchicago.edu>). The resultant HsIFN λ 4 structural model was then structurally aligned with both HsIFN λ 1 (PDB 3OG6) [38] and HsIFN λ 3 (PDB 5T5W) [39]. Visualization, structural alignments, and figures were generated in Pymol (The PyMOL Molecular Graphics System, Version 1.8).

Recombinant DNA manipulation and generation of IFN λ expression plasmids

DNA sequences encoding the ORFs of HsIFN λ 4, PtIFN λ 4 and MmIFN λ 4 (based on accession numbers above) were synthesized commercially with a carboxy-terminal DYKDDDDK/FLAG tag using GeneStrings or Gene Synthesis technology (GeneArt). As a positive control for

functional assays, the HsIFN λ 3 ORF was codon optimised (human) to ensure robust expression and antiviral activity, and is termed 'HsIFN λ 3op'; the exception to this were the HiBiT-tagged versions of HsIFN λ 3 which were not codon optimised. All IFN λ 4 coding region sequences were retained as the original nucleotide sequence without optimisation. Synthesized DNA was cloned into the pCI mammalian expression vectors (Promega) using standard molecular biology techniques. At each cloning step, the complete ORF was sequenced to ensure no spurious mutations had occurred during plasmid generation and manipulation. Single amino acid changes were incorporated using standard site-directed mutagenesis protocols (QuickChange site-directed mutagenesis kit [Agilent], or using overlapping oligonucleotides and Phusion PCR).

Cell lines and treatment with inhibitors of secretion

A549 (human lung adenocarcinoma), U2OS (human osteosarcoma), MDCK (Madin-Darby canine kidney) and HepaRG (non-differentiated human hepatic progenitor) cells were obtained from Chris Boutell; Huh7 (human hepatoma) cells were obtained from Charles Rice, Rockefeller University, USA; HEK293T (human embryonic kidney) cells were obtained from Sam Wilson; Vero (African Green Monkey kidney) cells were obtained from Arvind Patel. Cells were grown in DMEM growth media supplemented with 10% FBS and 1% penicillin-streptomycin except for HepaRG and genome-edited derivatives (generated during this study); these cells were cultured in William's E medium supplemented with 10% of FBS, 1% penicillin-streptomycin, hydrocortisone hemisuccinate (50 μ M) and human insulin (4 μ g/mL). Huh7 cells harbouring the HCV JFH-1 sub-genomic replicon [Tri-JFH1; 32] were cultured in the presence of 500 μ g/ml G418. All cells were grown at 37°C with 5% CO₂. Cell lines were routinely tested for mycoplasma and no contamination was detected.

To inhibit secretion of HsIFN λ s, cells were treated with BFA and Monensin at a final concentration of 5 μ g/ml. BFA was purchased in DMSO-dissolved form (10 mg/ml) and Monensin sodium salt was dissolved in methanol to the same concentration as BFA; both inhibitors were purchased from Sigma-Aldrich (UK).

Plasmid transfection and production of functional IFN λ

Plasmid DNA generated from bacterial cultures (GeneJET plasmid midiprep kit, ThermoScientific) was introduced into cells by lipid-based transfection using Lipofectamine 2000 or Lipofectamine 3000 (ThermoFisher) following manufacturer's instructions. To produce IFN-containing conditioned media (CM) or measure protein production, HEK293T 'producer' cells were grown to near-confluency in 12 (~4 x 10⁵ cells per well) or 6-well (~1.2 x 10⁶ cells per well) plates and transfected with plasmids (2 μ g) in OptiMEM (1–2 ml) overnight. At approximately 16 hours (hrs) post transfection (hpt), OptiMEM was removed and replaced with complete growth media (1–2 ml). CM containing the extracellular IFN λ s was harvested at 48 hpt and stored at -20°C before use. Although antiviral activity was observed at 16 hpt, we chose 48 hpt to harvest CM to ensure robust production and secretion of each IFN λ . Intracellular IFN λ s also were harvested from transfected cells at 48 hpt. CM was removed and replaced with fresh DMEM 10% FCS (2 ml) and then frozen at -70°C. To prepare cell lysates with IFN λ activity, plates were thawed and the cell monolayer was scraped into the media and clarified by centrifugation (5 minutes [mins] x 300 g) before use. CM or lysates were diluted in the respective growth medium for each cell line before functional testing as described in the text. Two-fold serial dilutions of CM were used in titration of anti-EMCV activity and ability to induce EGFP in an IFN-reporter cell line. Single CM dilutions of 1:4 (HepaRG and A549) or 1:3

(Huh7) were chosen based on initial experiments for gene expression and non-EMCV antiviral activity measurements to allow measurement of both high and low activity variants.

FLAG-immunoprecipitation

Immunoprecipitation of extracellular FLAG-tagged IFN λ 4 present in the supernatant of transfected cells was carried out using an anti-FLAG M2 antibody-bound gel as described by the manufacturer's guidelines (Sigma Aldrich). Immunoprecipitated IFNs were used in activity assays and for Western blot analysis. Briefly, resin with anti-FLAG antibody (40 μ l) and supernatants (1 ml) were thawed on ice. Beads were washed repeatedly in ice cold buffer before being incubated with IFNs in CM for 2 hrs at 4°C while rocking. Bead-bound IFN was pelleted by centrifugation, washed and eluted with FLAG peptide (100 μ l). Positive and negative controls were 'BAP-FLAG' and buffer only, respectively. Centrifugation conditions were 8,200 x g for 30 sec at 4°C. One quarter (25 μ l) of total immunoprecipitated protein was loaded onto gels for Western blot analysis.

Split NanoLuc complementation assay for measuring IFN production and secretion

The FLAG tag at the C-terminal ends of IFN λ s was replaced with the 11 amino acid HiBiT tag without a linker (amino acid sequence: N-VSGWRLFKKIS-C [41]) using PCR and subsequent cloning into the pC1 vector. To block secretion from cells, the first 26 amino acids of HsIFN λ 3 and 23 amino acids of HsIFN λ 4, corresponding to their respective N-terminal signal peptide sequences, were removed using a similar approach. The sequences of all plasmid constructs were verified. Luciferase activity was measured following transfection of plasmids using the Nano-Glo HiBiT Lytic Detection System and its Extracellular Detection System counterpart following manufacturers protocols (Promega, UK). Briefly, for measuring intracellular enzyme activity, supernatant was removed from transfected cells and lytic buffer was added directly to the cell monolayer before incubation for 10 minutes; all lysed material was transferred to a 1.5 ml Eppendorf tube and luciferase activity was measured in a luminometer. For determining extracellular activity, 100 μ l of the CM was removed from the culture medium and mixed 1:1 with both the LgBiT and substrate for 10 minutes prior to measuring luciferase activity; the luciferase value for secreted HiBiT-tagged HsIFN λ was then calculated based on the total volume of culture medium. Ratios to determine the extent of secretion of each IFN λ were generated based on total intracellular and extracellular luciferase values.

Relative quantification of RNA by reverse transcriptase-quantitative polymerase chain reaction (RT-qPCR)

Total cellular RNA was isolated by column-based guanidine thiocyanate extraction using RNeasy Plus Mini kit (genomic DNA removal 'plus' kit, Qiagen) according to the supplier's protocol. cDNA was synthesised by reverse transcribing RNA (1 μ g) using random primers and the AccuScript High Fidelity Reverse Transcriptase kit (Agilent Technologies); the recommended protocol was followed. Relative expression of mRNA was quantified by qPCR (7500 Real-Time PCR System, Applied Biosystems) of amplified cDNA. Probes for *ISG15* (Hs01921425), *Mx1* (Hs00895608) and the control *GAPDH* (402869) were used with TaqMan Fast Universal PCR Master Mix (Applied Biosystems). The results were normalised to *GAPDH* and presented in $2^{-\Delta\Delta C_t}$ values relative to controls as described in the text. HCV genomic RNA was quantified by RT-qPCR as described previously [32].

Global transcriptomic measurements and pathway analysis

IFN-competent cells (A549) were stimulated with IFN CM (1:4 dilution) in 6-well plates ($\sim 1.2 \times 10^6$ cells) for 24 hrs and global gene expression was assessed by RNA-Seq, using three biological replicates per condition. Sample RNA concentration was measured with a Qubit Fluorometer (Life Technologies) and RNA integrity (RIN) was determined using an Agilent 4200 TapeStation. All samples had a RIN value of 9 or above. 1.5 μ g of total RNA from each sample was prepared for sequencing using an Illumina TruSeq Stranded mRNA HT kit according to the manufacturer's instructions. Briefly, polyadenylated RNA molecules were captured, followed by fragmentation. RNA fragments were reverse transcribed and converted to dsDNA, end-repaired, A-tailed, ligated to indexed adaptors and amplified by PCR. Libraries were pooled in equimolar concentrations and sequenced in an Illumina NextSeq 500 sequencer using a high output cartridge, generating approximately 25 million reads per sample, with a read length of 75 bp. 96.3% of the reads had a Q score of 30 or above. Data was de-multiplexed and fastq files were generated on a bio-linux server using bcl2fastq version v2.16. RNA-Seq analysis was performed using the Tuxedo protocol [63]. Briefly, reads from 3 replicates per condition were aligned and junctions mapped against the human reference transcriptome hg38 using Tophat2 with the default settings except library type. Transcriptome assembly was performed using Cufflinks supplying annotations from the reference genome hg38 and the differential gene expression was calculated using Cuffdiff. Differential gene expression was considered significant when the observed fold change was ≥ 2.0 and FDR/q-value was < 0.05 between comparisons. Pathway analysis was carried out using Ingenuity Pathway Analysis [IPA] (Ingenuity Systems, Redwood City, CA, USA).

Western blot analysis

Cell growth media was removed and monolayers were rinsed once with approximately 0.5 ml PBS before lysis using RIPA buffer (ThermoFisher) containing protease inhibitor cocktail (1x Halt Protease inhibitor cocktail, ThermoFisher, or cOmplete, Mini, EDTA-free Protease Inhibitor Cocktail, Sigma Aldrich) for 10 mins at 4°C before being frozen at -20°C overnight. Lysates were collected into a 1.5 ml sample tube and clarified by centrifugation (12,000 x g for 15 mins). Samples (10 μ l) from the soluble fraction were heated to 90°C for 10 mins with 100 mM dithiothreitol (DTT)-containing reducing lane marker at 90°C for 10 mins. Samples were run on home-made 12% SDS-PAGE gels alongside molecular weight markers (Pierce Lane marker, ThermoFisher) before wet-transfer to nitrocellulose membrane. Membranes were blocked using a solution of 50% PBS and 50% FBS for 1 hr at room temperature and then incubated overnight at 4°C with primary antibodies in 50% PBS, 50% FBS and 0.1% TWEEN 20. Secondary antibodies were incubated in 50% PBS, 50% FBS and 0.1% TWEEN 20 for 1 hr at room temperature. Membranes were washed four times (5 mins each) following each antibody incubation with PBS containing 0.1% TWEEN 20. After the 4th wash following incubation with the secondary antibody, the membrane was washed once more in PBS (5 mins) and kept in ddH₂O until imaging. Primary antibodies to the FLAG tag (1:1000) (rabbit, lot. 064M4757V, LiCor) and α -tubulin (1:10000) (mouse, lot. GR252006-1, LiCor) were used along with infra-red secondary antibodies (LI-COR) to anti-rabbit (donkey [1:10,000], 926-68073) and anti-mouse (donkey [1:10,000], C50422-05) to allow protein visualisation. Pre-stained, PAGERuler Plus marker was used to determine molecular weights (ThermoFisher). Membranes were visualised using the LI-COR system on an Odyssey CLX and the relative expression level of proteins determined using LI-COR software (Image Studio).

Generation and use of IFN reporter cell lines

An IFN reporter HepaRG cell line was generated to measure IFN activity by introducing the EGFP ORF fused to the ISG15 ORF separated by ribosome skipping sites by CRISPR-Cas9 genome editing. We chose to introduce EGFP in-frame to the N-terminus of the *ISG15* ORF since it is a robustly-induced ISG. We also introduced the blasticidin resistance gene (BSD) for selection purposes. BSD, EGFP and *ISG15* were separated using ribosome skipping 2A sequences (P2A and T2A). Transgene DNA was flanked by homology arms with reference to the predicted target site. Homology donor plasmids for CRISPR-Cas9 knock-in were generated through a series of overlapping PCR amplifications using Phusion DNA polymerase followed by sub-cloning into pJET plasmid. Plasmids for CRISPR-Cas9 genome editing (wt SpCas9) were generated using established protocols [64] in order to create plasmids that would direct genome editing at the 5' terminus of the HsISG15 ORF (exon 2). pSpCas9(BB)-2A-Puro (PX459) V2.0 was a gift from Feng Zhang (Addgene plasmid # 62988). All sequences are available by request. HepaRG cells grown in 6 well dishes were co-transfected with CRISPR-Cas9 editing plasmids targeting the beginning of the *ISG15* ORF in exon 2 (exon 1 contains only the ATG of the ORF), and homology donor plasmids described above (1 µg each) using Lipofectamine 2000 and the protocol described above. Transfected cells were selected using puromycin (Life Technologies) (1 µg/ml) and blasticidin (Invivogen) (10 µg/ml) until non-transfected cells were no longer viable. Selected cells were cloned by single cell dilution, expanded and tested for EGFP induction following IFN stimulation. Positioning of the introduced transgene was assessed by PCR amplification on isolated genomic DNA from individual clones (S5C Fig). Primers were designed to include one primer internal to the transgene and another external to the transgene and found in the target loci (sequences available on request). For use as an effective IFN reporter cell line, cells had to demonstrate robust induction of EGFP expression following stimulation with IFN and evidence of specific introduction of the transgene. This study uses clone 'G8' of HepaRG.EGFP-BSD-*ISG15* cells. We have not tested whether there is a single transgene integration site or multiple ones nor confirmed that the EGFP produced following stimulation by IFNs results from the expression of the specifically-introduced transgene rather than off-target integration, which is theoretically possible. We do not predict this would affect the cells' ability to act as a reporter cell line. For use in IFN reporter assays, stimulated cells (in 96 well plates stimulated for 24 hrs; $\sim 5 \times 10^4$ cells per well) were washed, trypsinised and fixed in formalin (1% in PBS) at room temperature for 10 mins in the dark before being transferred to a round-bottomed plate and stored at 4°C in the dark until measurement of EGFP fluorescence. Non-stimulated cells were used as negative controls and the change in % EGFP-positive cells was assessed by flow cytometry using a Guava easy-Cyte HT (Merck Millipore). For fluorescence microscopy, EGFP induction was measured by indirect immunofluorescence of stimulated cells that were fixed and permeabilised on coverslips prior to antibody binding. An EGFP primary antibody (1:1000, rabbit ab290 Abcam) was used followed by a fluorescent anti-secondary antibody (1:500, Goat anti Rabbit Alexa-Fluor, Thermo Fisher, 568nm). Samples were counter-stained using DAPI and visualised with a confocal laser-scanning microscope (Zeiss LSM 710) under identical conditions.

Production of virus stocks for antiviral assays

Antiviral activity of IFN λ s was determined using encephalomyocarditis virus (EMCV), influenza A virus (IAV; A/WSN/1933(H1N1)), Zika virus (ZIKV; Brazilian strain PE243) [65] and HCV (HCVcc chimeric clone Jc1) [66]. EMCV was grown on Vero cells followed by titration on U2OS cells by plaque assay. IAV stocks were generated on MDCK cells and titrated by plaque assay on MDCK cells with protease (TPCK-treated trypsin, Sigma Aldrich). ZIKV was

titrated on Vero cells by plaque assay. For all plaque assays, cells were grown in 12 or 6-well plates to ~90% confluency before inoculation with serial 10-fold dilutions of virus stocks in serum-free Optimem. Inoculum remained on the cells for 2 hrs before removal and the monolayers were rinsed with PBS (1x) and semi-solid Avicell overlay (Sigma Aldrich) was added. For EMCV and IAV, 1.2% Avicell was used, diluted in 1x DMEM 10% FCS, 1% penicillin-streptomycin. For IAV titration, TPCK-treated trypsin was added (1 µg/ml). For ZIKV plaque assay, 2x MEM was used instead of 1x DMEM. HCVcc Jc1 was generated as described previously by electroporation of *in vitro* transcribed viral RNA into Huh7 cells and harvested at 72 hrs post electroporation. After filtration of the supernatant, HCVcc Jc1 stocks were titrated by TCID₅₀ on Huh7 cells and stored at 4°C before use. HCVcc Jc1 TCID₅₀ assays were performed using anti-NS5A antibody [67]. Infected cells at 72 hrs post infection were fixed and permeabilised with ice-cold methanol. Cells were rinsed in PBS, blocked with 3% FCS in PBS at room temperature and incubated overnight with mouse monoclonal anti-NS5A antibody (9E10) at 4°C. After removal of the antisera, cells were rinsed 3 times with PBS containing 0.1% TWEEN 20, and then incubated in the dark at room temperature for 1 hr with secondary antibody [Alexa-fluor 488nm anti-mouse (donkey)]. Cells were finally washed with PBS containing 0.1% TWEEN 20 and NS5A-expressing cells were visualized with a fluorescent microscope.

Antiviral assays

Cells stimulated with IFNλs were infected with viruses at the following multiplicities of infection (MOI): EMCV (MOI = 0.3; added directly to the media); IAV (MOI = 0.01); ZIKV (MOI = 0.01); HCVcc (MOI = 0.05). For IAV, ZIKV and HCVcc, the inoculum was incubated with cells for at 2 (IAV/ZIKV) or 3 hrs (HCVcc) in 0.5–1.0 ml serum-free Opti-MEM/DMEM at 37°C before removal. Cells were rinsed with PBS and then incubated with fresh growth media for the allotted time (24 hrs for EMCV, 48 hrs for IAV and 72 hrs for ZIKV and HCVcc). At the times stated for individual experiments, infected-cell supernatants were harvested and infectivity was titrated by plaque assay. IAV, ZIKV and HCVcc antiviral assays were all carried out in 12 well plates except for measurement of HCVcc infectivity by indirect immunofluorescence, which was measured in a 96 well plate. In the case of EMCV, a cytopathic effect (CPE) protection assay was employed to assess infectivity (26). Here, HepaRG cells were plated in a 96-well plates (~5 x 10⁴ cells per well) and, when confluent, were incubated with two-fold serial dilutions of CM or lysate for 24 hrs before the addition of EMCV. At 24 hrs post infection with EMCV, media was removed, cell monolayers were rinsed in PBS and stained using crystal violet (1% in 20% ethanol in H₂O) for 10 mins. Crystal violet stain was then removed and stained plates were washed in water. The dilution of ~50% inhibition of EMCV-induced CPE was marked visually and the difference determined relative to wt HsIFNλ4.

Luciferase-expressing MLV pseudoparticles containing the E1 and E2 glycoproteins from JFH1 HCV strain were generated as described [68] along with their corresponding JFH1 E1-E2 deficient controls (particles generated only with MLV core) and used to challenge IFNλ-stimulated Huh7 cells. Huh7 cells grown in 96-well plates overnight (seeded at 4 x 10³ cells per well) were stimulated with IFNλs for 24 hrs and transduced with HCVpp. 72 hrs later, cell lysates were harvested and luciferase activity was measured (Luciferase assay system, Promega) on a plate reading luminometer.

For HCV RNA replication assays, RNA was transcribed *in vitro* from a sub-genomic replicon (HCV-SGR) expressing GLuc (wild-type and non-replicating GND) [69]. *In vitro* transcribed RNA (200 ng) was transfected using PEI (1:1) into monolayers of Huh7 cells in 96-well

plates overnight (seeded at 4×10^3 cells per well) that had been stimulated with IFN λ s (24 hrs). At the specified time points, total supernatants (containing the secreted GLuc) from treated Huh7 cells were collected and replaced with fresh growth media. 20 μ l (~10% of total volume) was used to measure luciferase activity and mixed with GLuc substrate (1x) (50 μ l) and luminescence (as relative light units, RLUs) was determined using a luminometer (Promega Glo-Max). Pierce *Gaussia* Luciferase Flash Assay Kit (ThermoFisher) was used and the manufacturer's instructions were followed.

Comparison of human and chimpanzee intrahepatic gene expression during acute HCV infection

Previously published datasets of intrahepatic differentially-expressed genes from liver biopsies were used to compare human and chimpanzee transcriptomic responses to early HCV infection. At first, we used reported lists of differentially-expressed genes between humans and chimpanzees but further validated observations with raw data from human studies. Studies focusing on acute HCV infection (0 to 26 weeks) in humans and chimpanzees were acquired through manual literature search using Pubmed and gene lists were compiled. For chimpanzees, data was acquired from 4 studies [34–37] and one report was employed for human data [33]. The study by Dill et al. comprised single biopsy samples from each of six individuals, while *in toto* the chimpanzee studies combined data from ten animals with multiple, serial biopsies. All studies were carried out using similar Affymetrix microarray platforms except Nanda *et al.* who used IMAGE clone deposited arrays. Although similar microarrays measured different numbers of genes we focused on 'core' shared genes from chimpanzee studies. Humans were infected with HCV genotype (gt)1 (n = 2), gt3 (n = 3) and gt4 (n = 1) while chimpanzees were experimentally infected with HCV gt1a (n = 6), gt1b (n = 3) and gt2a (n = 1). The human dataset included individuals with IL28B rs12979860 genotypes T/T, C/T and C/C but no association between IL28B genotype and gene expression was noted (33). Gene names and fold-changes were manually converted to a single format (fold change rather than log₂ fold change for example) to allow comparative analysis. Human biopsies were taken between two and five months after presumed infection following known needle-stick exposure, and serial chimpanzee biopsies were taken at different time points from between one week and one year after HCV infection. For comparative purposes, differentially-expressed genes in chimpanzees were included if they were detected during a time period overlapping with the human data. We identified a 'core' set of chimpanzee differentially-expressed genes (independently characterized in at least two studies) and compared them to the single human transcriptome study data at equivalent time points (between 8 and 20 weeks post-infection). This approach generated a set of core chimpanzee genes (genes found differentially-expressed in at least 2 studies, >2 fold change compared to controls and during the time frame compared to humans) for comparison with the human data. This is reflected in the ten-fold higher numbers of differentially-regulated genes found in the one human study compared to the 'core' (reduced) set assembled from four chimpanzee studies. To validate these findings, we used three studies of chronic infection for which data were available [56,70,71], two from humans employing RNA-Seq and one from chimpanzees using microarray measurement. Gene lists were extracted and a core human list was produced and compared to that from chimpanzees. For shared genes, the fold change values were compared for humans and chimpanzees. The ratio of chimpanzee induction to human induction was calculated.

These gene sets were compared to determine their degree of species-specificity or species-similarity using Venn diagram analysis (<http://bioinfogp.cnb.csic.es/tools/venny/>). The gene lists for humans and core genes for chimpanzees are shown in the [S1 Data](#). For the

chimpanzee-biased genes, mean expression values were determined at each time point from individual animals.

Statistical analysis

For non-transcriptomic analysis (transcriptomic analysis is outlined above), Graphpad Prism was used for statistical testing, which included Students' T test and ANOVA and post-hoc tests (Dunnnett's test) where appropriate as described in figure legends. ****, $p = <0.0001$; ***, $p = <0.001$; **, $p = <0.01$; *, $p = <0.05$, are used throughout to denote statistical significance. Unless explicitly stated, in our analysis, the term biological replicate refers to measurements made from different wells during an experiment on the same day while independent experiment refers to measurements made from assays carried out on different days.

Ethics statement

Ethical approval was not required for analysis of human or animal samples as no such material was used in this study. All human and animal genomic and transcriptomic datasets were obtained from either publicly-available data or published data. We note that all data collected in the original studies was subject to ethical approval, details of which are available in the original study manuscripts.

Supporting information

S1 Fig. Non-synonymous variants of HsIFN λ 4 are located in regions of functional significance. (A) Schematic location of non-synonymous variants in the HsIFN λ 4 polypeptide (N- to C-terminus) (above schematic in pink). Regions of predicted structural significance are underlined, including the signal peptide (SP), single N-linked glycosylation site (N-glyc, arrowed), helices (A to F) and disulphide bonds (C-C). Note that there are 2 non-synonymous changes at C17 (C17R and C17Y). Helices involved in receptor interactions (IL10R2 and IFN λ R1) are highlighted. (B and C) Location of non-synonymous variants on a homology model of HsIFN λ 4 (side chains in colour) from two perspectives. Model was generated using the SWISS-MODEL online software. Helices are labelled A to F. Positions are coloured based on spatial clustering in the primary amino acid sequence. (TIF)

S2 Fig. Rare non-synonymous variants of HsIFN λ 4 affect antiviral activity. For data shown in panels A-D, all naturally-occurring variants of HsIFN λ 4 were tested in antiviral and ISG induction assays. Experimental conditions included a series of controls including HsIFN λ 3op (positive control), EGFP and the HsIFN λ 4 TT variant (negative controls) as well as non-natural variants of HsIFN λ 4 (N61A, F159A, L162A). N61A abrogates glycosylation of HsIFN λ 4 while F159A and L162A are predicted to reduce interaction with the IFN λ R1 receptor subunit and hence lower activity based on previous studies [27]. Panels show data from the following assays: (A) Antiviral activity in an anti-EMCV CPE assay in HepaRG cells. Cells were stimulated with serial dilutions of HsIFN λ 4-containing CM for 24 hrs and then infected with EMCV (MOI = 0.3 PFU/cell) for 24 hrs at which point CPE was assessed by crystal violet staining. After staining, the dilution providing ~50% protection was determined. Data are shown as mean +/- SD of three independent experiments performed on different days. (B and C) ISG gene expression determined by RT-qPCR following stimulation of cells with HsIFN λ 4 variants. Relative fold change of *ISG15* mRNA (B) or *Mx1* (C) in HepaRG cells stimulated with CM (1:4 dilution) from plasmid-transfected cells compared to wt HsIFN λ 4. Cells were stimulated for 24 hrs. Error bar represent mean +/- SD of biological replicates (n = 3). (D) Western

blot analysis of unconjugated and high molecular weight conjugated-forms of ISG15 ('ISGylation') from lysates harvested from HepaRG cells stimulated with CM (1:4) for 24 hrs. (TIF)

S3 Fig. Relative expression of glycosylated and non-glycosylated forms of HsIFNλ4 variants.

For data in panels A and B, expression and glycosylation of all naturally-occurring variants of HsIFNλ4 were examined. Experiments included a series of controls including HsIFNλ3op (contains no glycosylation sites), EGFP and the HsIFNλ4 TT variant (negative controls) as well as non-natural variants of HsIFNλ4 (N61A, F159A, L162A). N61A is predicted to abrogate glycosylation of HsIFNλ4. Panel A shows a representative Western blot for the production and glycosylation of HsIFNλ4 variants of lysates from plasmid-transfected producer HEK293T cells as detected with an anti-FLAG ('FLAG') primary antibody. Tubulin was used as a loading control. A non-specific band in the EGFP-transfected extract is shown (*). Panel B shows the quantification of intracellular glycosylated (green) and non-glycosylated (blue) HsIFNλ4 variants by Western blot analysis of lysates from plasmid-transfected producer HEK293T cells. Ratio of glycosylated to non-glycosylated is shown above the graph. Two-fold differences from wild-type are highlighted in bold. Data shown are mean +/- SEM combined from three independent experiments. (TIF)

S4 Fig. Presence of HsIFNλ4 K154E variant in Pygmies and evolution of HsIFNλ4 variants in human populations.

(A) Geographical location and frequency of HsIFNλ4 K154E in African hunter-gatherer alleles (Pygmy, n = 5 individuals, Sandawe (S) n = 5 individuals and Hadza (H) n = 5 individuals). Two Pygmy individuals within two tribes (Baka and Bakola) were found to encode the HsIFNλ4 K154E variant. The proportion of ΔG (red) and TT (blue) *IFNL4* alleles are also shown in pie-charts. (B) Presence of HsIFNλ4 E154 (purple) versus HsIFNλ4 K154 (green) on a cladogram of human and chimpanzee evolution. Archaic human (Neanderthal and Denisovan) as well as other basal human populations (San, Sandawe and Hadza) only encode HsIFNλ4 K154. Earliest detection of the HsIFNλ4 TT frameshift and activity-reducing HsIFNλ4 P70S and HsIFNλ4 L79F variants are shown. All analysis can be found in [S1 Data](#). (TIF)

S5 Fig. Generation of a reporter HepaRG cell line expressing EGFP in the ISG15 promoter region.

(A) Strategy for CRISPR-Cas9 genome editing combined with homologous recombination insertion of DNA sequences to produce an EGFP-expressing ISG15 promoter cell line. The strategy enables the insertion of a cassette in-frame with the ISG15 ORF that encodes blasticidin resistance (BSD) and EGFP genes followed by *ISG15*, separated by '2A' ribosomal skipping sequences. Target gDNA and CRISPR-Cas9 cut sites are shown on the upper cartoon. Binding sites of primers for genotyping are highlighted (+) and (-) in the resulting modified gDNA. (B) Induction of EGFP expression (green immunofluorescence) in the G8 cell clone with or without treatment with PolyI:C (1.0 μg/ml for 24 hrs). Poly(I:C) stimulates the Toll-like receptor TLR3, which induces ISG15 expression. Cells were fixed in formalin, permeabilised and stained for indirect immunofluorescence with an anti-EGFP primary antibody before addition of a secondary antibody. DAPI was used as a counter stain for cell nuclei. (C) Cell line clone (G8) used for reporter assays was validated by PCR analysis yielding an amplified DNA fragment of ~1000 bp from primers located in *ISG15* and EGFP sequences. (TIF)

S6 Fig. Serial passaging of stable HCV SGR-bearing cells in the presence of HsIFNλ4.

(A) A schematic of the experiment showing passaging of Tri-JFH1 Huh7 cells in the presence of

HsIFN λ 4 is shown. (B) Briefly, Tri-JFH1 cells were treated with CM containing wt HsIFN λ 4 or HsIFN λ 4 K154E alongside a negative control (EGFP) at a dilution of 1:2 for three days before repeat passaging at a ratio of 1:6 into EGFP- or HsIFN λ 4-containing CM, again at a 1:2 dilution. This treatment and passaging were repeated 8 times over a total of 25 days. Cells were grown in 6 well plates. At each passage, a proportion of cells was stored for RNA extraction and quantification of HCV SGR RNA levels by RT-qPCR. HCV RNA relative to GAPDH was quantified for wt (orange) and K154E (purple) HsIFN λ 4-treated cells, and expressed relative to the amount of RNA in the paired EGFP-treated cells. The arrow indicates a stage in the experiment where the cells were incubated for 4 instead of 3 days and reached confluency, which likely reduced HCV replication. The data show the mean and SD of biological duplicates. (C) At the end of the experiment (P8, 25 days), the cells were plated into a 96 well plate without either wt or K154E HsIFN λ 4 and then fixed the following day in ice-cold methanol prior to staining for HCV NS5A antigen by indirect immunofluorescence to determine the number of cells harbouring replicating HCV RNA. Representative fluorescence microscopy and brightfield images are shown. Scale bars represent 400 μ m. (TIF)

S7 Fig. Comparative induction of hepatic transcripts during acute HCV infection in chimpanzees and humans. (A) Expression of ‘chimpanzee-biased’ differentially-expressed genes ($n = 29$) up to more than 50 weeks post infection. Chimpanzee-biased genes are shown as a combined mean (filled orange line) and range (dotted orange lines) of fold-change from all studies where any gene of the 29 genes was available over at most 1 year after initial infection. (B) Expression of differentially-expressed human and chimpanzee genes during 8 to 20 weeks post infection. Chimpanzee-biased genes are shown as a combined mean (filled orange line) and range (dotted orange lines) of fold-change from all 29 genes. The mean and range of gene expression for the human genes (blue filled and dotted lines respectively) equivalent to the chimpanzee-biased genes are shown. These data for chimpanzees are combined from different serial samples from different animals while human data is taken from a single biopsy from patients with an inferred time post infection. (C) Shared gene expression (overlapping 44 genes as shown in Venn diagram) during chronic infection in humans and chimpanzees as illustrated by a ratio of fold change in expression for humans and chimpanzees. Species biased genes (>2 fold enriched in either species) are listed to the side. All data are available in [S3 Data](#). (TIF)

S8 Fig. Structural modelling of P70 and L79 in HsIFN λ 4. Modelled structures of HsIFN λ 4 (light blue) are overlaid on the crystal structures for HsIFN λ 1 (green) and HsIFN λ 3 (dark blue). Panels A and B show respectively positions P70 and L79 in HsIFN λ 4 and their homologous positions in HsIFN λ 1 and HsIFN λ 3 with reference to receptor subunit-binding interfaces (IFN λ R1 and IL10R2 in grey). (A) P70 is found in a flexible proline-rich loop/helix facing the IFN λ R1 receptor although no direct interactions between this region or receptor have been demonstrated. P70S might prevent required folding of the protein domain. (B) L79F is likely to disrupt packaging of the helices. Both P70 and L79 are highly conserved between IFN λ 4 orthologues and paralogues (31). (TIF)

S9 Fig. Mechanistic insight into variant E154. (A) Dilutions for inducing ~50% EGFP positive cells for HsIFN λ 4 IFN λ 4 154 mutants (R, L, A, D, E and Q) using an EGFP-ISG15 reporter cell line assay relative to CM for HsIFN λ 4 K154 (%). Data show mean \pm SEM from three independent experiments performed on different days. (B) Antiviral activity of HsIFN λ 4

isolated from CM (purple), intracellular lysate (blue) and immunoprecipitated CM (orange) for variants encoding E, K, R or D at position 154 in an anti-EMCV CPE assay relative to CM for wt HsIFN λ 4 (K154 variant) in HepaRG cells. (C) Detection of intracellular IFN λ 4 from different species as well as select mutants at position 154 (E, K, D and R) by Western blot analysis of lysates from plasmid-transfected producer HEK293T cells. The IFN λ 4 variants were detected with an anti-FLAG antibody. Tubulin was used as a loading control. These samples were taken from the same experiment as in Fig 6E. A lower molecular weight product detected by the anti-FLAG antibody, which is potentially a degradation product, is highlighted with a '#' (D) Alternative images from repeats of detection of extracellular IFN λ 4 from different species by Western blot analysis of samples of FLAG-tag immunoprecipitated CM (1 ml) from plasmid-transfected producer HEK293T cells. A BAP-FLAG fusion protein was used as an immunoprecipitation control (POS). IFN λ 4 variants were detected with an anti-FLAG antibody. A lower molecular weight product detected by the anti-FLAG antibody, which is potentially a degradation product, is highlighted with a '#'. An upper band running near to the IFN λ 4 species is shown (*) which is likely antibody fragments from the immunoprecipitation reaction. (E) Ratio of E154 to K154 for antiviral activity (all) or protein amounts (IP or LYS) of IFN λ 4 found in CM, intracellular lysate and immunoprecipitated CM; where possible, data from the different species is combined. Data show median +/- minimum and maximum (n = 6–8).

(TIF)

S10 Fig. Screening of secretion and potency of HsIFN λ 4 variants with the NanoLuc system.

(A) Relative light unit (RLU) values, minus background measurements, for intracellular (blue) and extracellular HsIFN λ s (red) as well as the ratios for these values (green) are shown relative to wt HsIFN λ 4 enzyme activity for all natural HsIFN λ 4 coding variants. Additional N61A (for HsIFN λ 4) and Δ SP controls (Δ SP3 and Δ SP4 for HsIFN λ 3 and HsIFN λ 4 respectively) were included in the screen. Dashed lines indicate two-fold differences and variants giving values outside of these margins are illustrated. The data represent the mean of three independent experiments performed on different days. (B) RLU values as a validation experiment from the screen in (A) are shown following the same colour scheme for select variants of interest, including R60P, P70S, L79F, K154E and V158I. The wt value is marked time with a dashed line. (C) Paired antiviral activity for samples presented in B is shown (purple squares) relative to wt HsIFN λ 4 alongside the respective amounts added (based on luciferase activity and relative to wt HsIFN λ 4). A higher relative antiviral activity compared to luciferase activity indicates higher potency while the reverse is true for less potent IFN λ s. The limit of detection is indicated for the antiviral activity assay (purple hashed line). The data shown in B and C represent mean and SD of biological duplicates.

(TIF)

S11 Fig. Inhibition of IFN λ secretion with inhibitors of the ER and Golgi secretion pathways.

Raw total RLU values minus the mock treated from within (A) and outside (B) the cell are shown following treatment of transfected cells with two inhibitors of the secretion pathway, brefeldin A (BFA) and monensin (Mo); appropriate negative controls using DMSO and methanol respectively for each compound are shown. Both inhibitors were used at a final concentration of 5 μ g/ml. HEK-293T cells transfected with plasmids were treated with inhibitors and controls at ~18 hpt and incubated for a further 24 hrs in the presence of the drug before luciferase activity were measured. In this experiment, wt HsIFN λ 3 and wt HsIFN λ 4 alongside the K154E variant and controls lacking the signal peptide sequence were used. (C) The extent of secretion for HsIFN λ s are shown as ratios of intracellular and extracellular luciferase values

from the experiment in A and B. Histograms show mean and SD from wells in triplicate. (TIF)

S12 Fig. Evolution and functional impact of variation at position 154 of IFN λ 4. (A) Inferred evolution of position 154 in humans and chimpanzees. The last common ancestor of humans and chimpanzees encoded the highly-conserved glutamic acid (E) at position 154 (purple). E154 was retained in chimpanzees but sequentially modified in the genus *Homo*, which includes humans and Neanderthals. *Homo* IFN λ 4 was first modified by substitution of E154 to lysine (K) (orange) and subsequent emergence of the frameshift TT allele (grey) or by the introduction of other substitutions that reduce activity (P70S [blue], L79F [yellow]). The TT allele also encodes the codon for K154. E154 (pink) re-emerged in Pygmies. IFN λ 4 in humans with only the E154K change remains in the population and is considered wild-type ('wt'). (B) Impact of E and K encoded at position 154 in IFN λ 4 on antiviral activity. Both IFN λ 4 E154 (purple) and K154 (orange) are produced and glycosylated (grey circle) to similar levels inside the cell but IFN λ 4 E154 is secreted more efficiently compared to IFN λ 4 K154 (highlighted by blue arrows) and has enhanced potency. Subsequently, IFN λ 4 E154 induces more robust interferon stimulated gene (ISG) expression (for example: *ISG15*, *IFIT1*, *MX1*) in target cells, leading to greater antiviral activity. (TIF)

S13 Fig. Validation of the L79F variant (rs564293856 G/A) by PCR and Sanger sequencing. (A) Chromatogram from an amplicon showing the region surrounding the rs564293856 variant for the American proband (NA19658) with no evidence of a G>A allele (highlighted with the vertical black arrow). (B) Chromatogram from an amplicon showing the region surrounding the rs564293856 variant for the African proband (HG03095) showing evidence for both G and A nucleotides at rs564293856 (highlighted with the vertical black arrow). This individual was heterozygous as predicted. (TIF)

S1 Data. Human genetic data for non-synonymous variants of IFNL4. The information provided include (i) complete SNP numbering, alleles and genotypes obtained from the 1000 Genomes Project Database, (ii) geographical/ethnic localisation of non-synonymous variants, and (iii) select genotypes for IFNL variants in African hunter-gatherers and Archaic human genomes. (XLSX)

S2 Data. Complete RNAseq gene expression analysis for A549 cells stimulated with IFN λ 4 variants. Details given include gene name, mean expression values, fold-changes and significance as well as tables of significant and >2-fold genes in each condition. (XLSX)

S3 Data. Analysis of differential gene expression in the livers of HCV-infected chimpanzees and humans. For acute values: the dataset includes gene lists and common and unique genes to each species for the complete data or for chimpanzees (all), those genes found in at least two studies to be differentially expressed (core); DAVID pathway analysis; comparison of in vivo and in vitro data from S2 Data along with numerical data of chimp-biased genes in humans and chimpanzees. Table also includes gene lists and fold-changes during chronic infection of up-regulated genes from humans and chimpanzees, how they are shared and, for the shared genes, the fold-change of expression in each species/condition, including HCV genotype, high or low ISG-induction status or chimpanzee identification number. (XLSX)

Acknowledgments

We are grateful to: Chris Boutell, Richard Elliott and Alain Kohl for IAV, EMCV and ZIKV respectively; Takaji Wakita, Ralf Bartenschlager and Arvind Patel for HCV reagents; Sam Wilson and Carol McWilliam Leitch for critically reading the manuscript.

Author Contributions

Conceptualization: Connor G. G. Bamford, John McLauchlan.

Data curation: Connor G. G. Bamford, Elihu Aranday-Cortes, Shaohua Fan.

Formal analysis: Connor G. G. Bamford, Elihu Aranday-Cortes, Juan L. Mendoza, Shaohua Fan, John McLauchlan.

Funding acquisition: Juan L. Mendoza, K. Christopher Garcia, Sarah A. Tishkoff, John McLauchlan.

Investigation: Connor G. G. Bamford, Elihu Aranday-Cortes, Ines Cordeiro Filipe, Swathi Sukumar, Daniel Mair, Ana da Silva Filipe, Juan L. Mendoza, Shaohua Fan.

Methodology: Connor G. G. Bamford, Elihu Aranday-Cortes, Ana da Silva Filipe.

Project administration: John McLauchlan.

Supervision: Connor G. G. Bamford, Ana da Silva Filipe, K. Christopher Garcia, Sarah A. Tishkoff, John McLauchlan.

Validation: Connor G. G. Bamford.

Visualization: Connor G. G. Bamford, Elihu Aranday-Cortes, John McLauchlan.

Writing – original draft: Connor G. G. Bamford, John McLauchlan.

Writing – review & editing: Connor G. G. Bamford, John McLauchlan.

References

1. Randall RE, Goodbourn S. Interferons and viruses: an interplay between induction, signalling, antiviral responses and virus countermeasures. *J Gen Virol.* 2008 89(1):1–47.
2. Schoggins JW, Wilson SJ, Panis M, Murphy MY, Jones CT, Bieniasz P, et al. A diverse range of gene products are effectors of the type I interferon antiviral response. *Nature.* 2011 472(7344):481–5. <https://doi.org/10.1038/nature09907> PMID: 21478870
3. Shaw AE, Hughes J, Gu Q, Behdenna A, Singer JB, Dennis T, et al. Fundamental properties of the mammalian innate immune system revealed by multispecies comparison of type I interferon responses. *PLOS Biol.* 2017 15(12):e2004086. <https://doi.org/10.1371/journal.pbio.2004086> PMID: 29253856
4. Schoggins JW. Interferon-stimulated genes: roles in viral pathogenesis. *Curr Opin Virol.* 2014 6C:40–6.
5. Kotenko S V., Gallagher G, Baurin V V., Lewis-Antes A, Shen M, Shah NK, et al. IFN-λs mediate antiviral protection through a distinct class II cytokine receptor complex. *Nat Immunol.* 2003 4(1):69–77. <https://doi.org/10.1038/ni875> PMID: 12483210
6. Sheppard P, Kindsvogel W, Xu W, Henderson K, Schlutsmeyer S, Whitmore TE, et al. IL-28, IL-29 and their class II cytokine receptor IL-28R. *Nat Immunol.* 2003 4(1):63–8. <https://doi.org/10.1038/ni873> PMID: 12469119
7. Nice TJ, Baldrige MT, McCune BT, Norman JM, Lazear HM, Artyomov M, et al. Interferon-λ cures persistent murine norovirus infection in the absence of adaptive immunity. *Science.* 2015 347(6219):269–73. <https://doi.org/10.1126/science.1258100> PMID: 25431489
8. Galani IE, Triantafyllia V, Eleminiadou E-E, Koltzida O, Stavropoulos A, Manioudaki M, et al. Interferon-λ mediates non-redundant front-line antiviral protection against influenza virus infection without compromising host fitness. *Immunity.* 2017 46(5):875–90.e6. <https://doi.org/10.1016/j.immuni.2017.04.025> PMID: 28514692

9. Lazear HM, Daniels BP, Pinto AK, Huang AC, Vick SC, Doyle SE, et al. Interferon- λ restricts West Nile virus neuroinvasion by tightening the blood-brain barrier. *Sci Transl Med*. 2015 7(284):284ra59. <https://doi.org/10.1126/scitranslmed.aaa4304> PMID: 25904743
10. Odendall C, Dixit E, Stavru F, Bierne H, Franz KM, Durbin AF, et al. Diverse intracellular pathogens activate type III interferon expression from peroxisomes. *Nat Immunol*. 2014 15(8):717–26. <https://doi.org/10.1038/ni.2915> PMID: 24952503
11. Espinosa V, Dutta O, McElrath C, Du P, Chang Y-J, Cicciarelli B, et al. Type III interferon is a critical regulator of innate antifungal immunity. *Sci Immunol*. 2017 2(16):eaan5357. <https://doi.org/10.1126/sciimmunol.aan5357> PMID: 28986419
12. Marcello T, Grakoui A, Barba-Spaeth G, Machlin ES, Kotenko S V., Macdonald MR, et al. Interferons α and λ inhibit hepatitis C virus replication with distinct signal transduction and gene regulation kinetics. *Gastroenterology*. 2006 131(6):1887–98. <https://doi.org/10.1053/j.gastro.2006.09.052> PMID: 17087946
13. Sommereyns C, Paul S, Staeheli P, Michiels T. IFN-lambda (IFN-lambda) is expressed in a tissue-dependent fashion and primarily acts on epithelial cells in vivo. *PLoS Pathog*. 2008 4(3):e1000017. <https://doi.org/10.1371/journal.ppat.1000017> PMID: 18369468
14. Lazear HM, Nice TJ, Diamond MS. Interferon- λ : Immune functions at barrier surfaces and beyond. *Immunity*. 2015 43(1):15–28. <https://doi.org/10.1016/j.immuni.2015.07.001> PMID: 26200010
15. Manry J, Laval G, Patin E, Fornarino S, Itan Y, Fumagalli M, et al. Evolutionary genetic dissection of human interferons. *J Exp Med*. 2011 208(13):2747–59. <https://doi.org/10.1084/jem.20111680> PMID: 22162829
16. Thomas DL, Thio CL, Martin MP, Qi Y, Ge D, O’Hugin C, et al. Genetic variation in IL28B and spontaneous clearance of hepatitis C virus. *Nature*. 2009 461(7265):798–801. <https://doi.org/10.1038/nature08463> PMID: 19759533
17. Ge D, Fellay J, Thompson AJ, Simon JS, Shianna K V., Urban TJ, et al. Genetic variation in IL28B predicts hepatitis C treatment-induced viral clearance. *Nature*. 2009 461(7262):399–401. <https://doi.org/10.1038/nature08309> PMID: 19684573
18. Prokunina-Olsson L, Muchmore B, Tang W, Pfeiffer RM, Park H, Dickensheets H, et al. A variant upstream of IFNL3 (IL28B) creating a new interferon gene IFNL4 is associated with impaired clearance of hepatitis C virus. *Nat Genet*. 2013 45(2):164–71. <https://doi.org/10.1038/ng.2521> PMID: 23291588
19. O’Brien TR, Pfeiffer RM, Paquin A, Lang Kuhs KA, Chen S, Bonkovsky HL, et al. Comparison of functional variants in IFNL4 and IFNL3 for association with HCV clearance. *J Hepatol*. 2015 63(5):1103–10. <https://doi.org/10.1016/j.jhep.2015.06.035> PMID: 26186989
20. Key FM, Peter B, Dennis MY, Huerta-Sánchez E, Tang W, Prokunina-Olsson L, et al. Selection on a variant associated with improved viral clearance drives local, adaptive pseudogenization of interferon lambda 4 (IFNL4). *PLoS Genet*. 2014 10(10):e1004681. <https://doi.org/10.1371/journal.pgen.1004681> PMID: 25329461
21. Hong M, Schwerk J, Lim C, Kell A, Jarret A, Pangallo J, et al. Interferon lambda 4 expression is suppressed by the host during viral infection. *J Exp Med*. 2016 213(12):2539–52. <https://doi.org/10.1084/jem.20160437> PMID: 27799623
22. Terczyńska-Dyla E, Bibert S, Duong FHT, Krol I, Jørgensen S, Collinet E, et al. Reduced IFN λ 4 activity is associated with improved HCV clearance and reduced expression of interferon-stimulated genes. *Nat Commun*. 2014 5:5699. <https://doi.org/10.1038/ncomms6699> PMID: 25534433
23. Auton A, Abecasis GR, Altshuler DM, Durbin RM, Abecasis GR, Bentley DR, et al. A global reference for human genetic variation. *Nature*. 2015 526(7571):68–74. <https://doi.org/10.1038/nature15393> PMID: 26432245
24. Hamming OJ, Terczyńska-Dyla E, Vieyres G, Dijkman R, Jørgensen SE, Akhtar H, et al. Interferon lambda 4 signals via the IFN λ receptor to regulate antiviral activity against HCV and coronaviruses. *EMBO J*. 2013 32(23):3055–65. <https://doi.org/10.1038/emboj.2013.232> PMID: 24169568
25. Luangsay S, Ait-Goughoulte M, Michelet M, Floriot O, Bonnin M, Gruffaz M, et al. Expression and functionality of Toll- and RIG-like receptors in HepaRG cells. *J Hepatol*. 2015 63(5):1077–85. <https://doi.org/10.1016/j.jhep.2015.06.022> PMID: 26144659
26. Mohamed M, McLees A, Elliott RM. Viruses in the Anopheles A, Anopheles B, and Tete serogroups in the Orthobunyavirus genus (family Bunyaviridae) do not encode an NSs protein. *J Virol*. 2009 83(15):7612–8. <https://doi.org/10.1128/JVI.02080-08> PMID: 19439468
27. Gad HH, Dellgren C, Hamming OJ, Vends S, Paludan SR, Hartmann R. Interferon- λ is functionally an interferon but structurally related to the interleukin-10 family. *J Biol Chem*. 2009 284(31):20869–75. <https://doi.org/10.1074/jbc.M109.002923> PMID: 19457860

28. Lachance J, Vernot B, Elbers CC, Ferwerda B, Froment A, Bodo J-M, et al. Evolutionary history and adaptation from high-coverage whole-genome sequences of diverse African hunter-gatherers. *Cell*. 2012 150(3):457–69. <https://doi.org/10.1016/j.cell.2012.07.009> PMID: 22840920
29. Lek M, Karczewski KJ, Minikel EV, Samocha KE, Banks E, Fennell T, et al. Analysis of protein-coding genetic variation in 60,706 humans. *Nature*. 2016 536(7616):285–91. <https://doi.org/10.1038/nature19057> PMID: 27535533
30. Mallick S, Li H, Lipson M, Mathieson I, Gymrek M, Racimo F, et al. The Simons Genome Diversity Project: 300 genomes from 142 diverse populations. *Nature*. 2016 538(7624):201–6. <https://doi.org/10.1038/nature18964> PMID: 27654912
31. Paquin A, Onabajo OO, Tang W, Prokunina-Olsson L. Comparative functional analysis of 12 mammalian IFN- λ 4 orthologs. *J Interf Cytokine Res*. 2016 36(1):30–6.
32. Jones DM, Domingues P, Targett-Adams P, McLauchlan J. Comparison of U2OS and Huh-7 cells for identifying host factors that affect hepatitis C virus RNA replication. *J Gen Virol*. 2010 91(9):2238–48.
33. Dill MT, Makowska Z, Duong FHT, Merkofer F, Filipowicz M, Baumert TF, et al. Interferon- γ -stimulated genes, but not USP18, are expressed in livers of patients with acute hepatitis C. *Gastroenterology*. 2012 143(3):777–86.e6. <https://doi.org/10.1053/j.gastro.2012.05.044> PMID: 22677194
34. Nanda S, Havert MB, Calderón GM, Thomson M, Jacobson C, Kastner D, et al. Hepatic transcriptome analysis of hepatitis C virus infection in chimpanzees defines unique gene expression patterns associated with viral clearance. *PLoS One*. 2008 3(10):e3442. <https://doi.org/10.1371/journal.pone.0003442> PMID: 18927617
35. Bigger CB, Brasky KM, Lanford RE. DNA Microarray analysis of chimpanzee liver during acute resolving hepatitis C virus infection. *J Virol*. 2001 75(15):7059–66. <https://doi.org/10.1128/JVI.75.15.7059-7066.2001> PMID: 11435586
36. Su AI, Pezacki JP, Wodicka L, Brideau AD, Supekova L, Thimme R, et al. Genomic analysis of the host response to hepatitis C virus infection. *Proc Natl Acad Sci*. 2002 99(24):15669–74. <https://doi.org/10.1073/pnas.202608199> PMID: 12441396
37. Yu C, Boon D, McDonald SL, Myers TG, Tomioka K, Nguyen H, et al. Pathogenesis of hepatitis E virus and hepatitis C virus in chimpanzees: similarities and differences. *J Virol*. 2010 84(21):11264–78. <https://doi.org/10.1128/JVI.01205-10> PMID: 20739520
38. Miknis ZJ, Magracheva E, Li W, Zdanov A, Kottenko S V., Wlodawer A. Crystal Structure of human interferon- λ 1 in complex with its high-affinity receptor interferon- λ R1. *J Mol Biol*. 2010 404(4):650–64. <https://doi.org/10.1016/j.jmb.2010.09.068> PMID: 20934432
39. Mendoza JL, Schneider WM, Hoffmann H-H, Vercauteren K, Jude KM, Xiong A, et al. The IFN- λ -IFN- λ R1-IL-10R β complex reveals structural features underlying type III IFN functional plasticity. *Immunity*. 2017 46(3):379–92. <https://doi.org/10.1016/j.immuni.2017.02.017> PMID: 28329704
40. Lu Y-F, Goldstein DB, Urban TJ, Bradrick SS. Interferon- λ 4 is a cell-autonomous type III interferon associated with pre-treatment hepatitis C virus burden. *Virology*. 2015 476:334–40. <https://doi.org/10.1016/j.virol.2014.12.020> PMID: 25577150
41. Dixon AS, Schwinn MK, Hall MP, Zimmerman K, Otto P, Lubben TH, et al. NanoLuc complementation reporter optimized for accurate measurement of protein interactions in cells. *ACS Chem. Biol*. 2016 11(2):400–8. <https://doi.org/10.1021/acschembio.5b00753> PMID: 26569370
42. Patterson N, Richter DJ, Gnerre S, Lander ES, Reich D. Genetic evidence for complex speciation of humans and chimpanzees. *Nature*. 2006 441(7097):1103–8. <https://doi.org/10.1038/nature04789> PMID: 16710306
43. Green RE, Krause J, Briggs A. W, Maricic T, Stenzel U, Kircher M, et al. A Draft sequence of the neanderthal genome. *Science*. 2010 328(5979):710–22. <https://doi.org/10.1126/science.1188021> PMID: 20448178
44. Cohen TS, Prince AS. Bacterial pathogens activate a common inflammatory pathway through IFN α regulation of PDCD4. *PLoS Pathog*. 2013 9(10):e1003682. <https://doi.org/10.1371/journal.ppat.1003682> PMID: 24098127
45. Mulangu S, Borchert M, Paweska J, Tshomba A, Afounde A, Kulidri A, et al. High prevalence of IgG antibodies to Ebola virus in the Efé pygmy population in the Watsa region, Democratic Republic of the Congo. *BMC Infect Dis*. 2016 16(1):263.
46. Bukh J. A critical role for the chimpanzee model in the study of hepatitis C. *Hepatology*. 2004 39(6):1469–75. <https://doi.org/10.1002/hep.20268> PMID: 15185284
47. Bassett SE, Brasky KM, Lanford RE. Analysis of hepatitis C virus-inoculated chimpanzees reveals unexpected clinical profiles. *J Virol*. 1998 72(4):2589–99. PMID: 9525575
48. Walker CM. Comparative features of hepatitis C virus infection in humans and chimpanzees. *Springer Semin Immunopathol*. 1997 19(1):85–98. PMID: 9266633

49. Lanford RE, Guerra B, Bigger CB, Lee H, Chavez D, Brasky KM. Lack of response to exogenous interferon- α in the liver of chimpanzees chronically infected with hepatitis C virus. *Hepatology*. 2007 46(4):999–1008. <https://doi.org/10.1002/hep.21776> PMID: 17668868
50. Ray SC, Mao Q, Lanford RE, Bassett S, Laeyendecker O, Wang YM, et al. Hypervariable region 1 sequence stability during hepatitis C virus replication in chimpanzees. *J Virol*. 2000 74(7):3058–66. PMID: 10708420
51. Eslam M, Hashem AM, Leung R, Romero-Gomez M, Berg T, Dore GJ, et al. Interferon- λ rs12979860 genotype and liver fibrosis in viral and non-viral chronic liver disease. *Nat Commun*. 2015 6:6422. <https://doi.org/10.1038/ncomms7422> PMID: 25740255
52. Ansari MA, Pedergrana V, L C Ip C, Magri A, Von Delft A, Bonsall D, et al. Genome-to-genome analysis highlights the effect of the human innate and adaptive immune systems on the hepatitis C virus. *Nat Genet*. 2017 49(5):666–73. <https://doi.org/10.1038/ng.3835> PMID: 28394351
53. Thomas E, Gonzalez VD, Li Q, Modi AA, Chen W, Noureddin M, et al. HCV infection induces a unique hepatic innate immune response associated with robust production of type III interferons. *Gastroenterology*. 2012 142(4):978–88. <https://doi.org/10.1053/j.gastro.2011.12.055> PMID: 22248663
54. Park H, Serti E, Eke O, Muchmore B, Prokunina-Olsson L, Capone S, et al. IL-29 is the dominant type III interferon produced by hepatocytes during acute hepatitis C virus infection. *Hepatology*. 2012 56(6):2060–70. <https://doi.org/10.1002/hep.25897> PMID: 22706965
55. Sheahan T, Imanaka N, Marukian S, Dorner M, Liu P, Ploss A, et al. Interferon lambda alleles predict innate antiviral immune responses and hepatitis C virus permissiveness. *Cell Host Microbe*. 2014 15(2):190–202. <https://doi.org/10.1016/j.chom.2014.01.007> PMID: 24528865
56. Boldanova T, Suslov A, Heim MH, Necseulea A. Transcriptional response to hepatitis C virus infection and interferon-alpha treatment in the human liver. *EMBO Mol Med*. 2017 9(6):816–34. <https://doi.org/10.15252/emmm.201607006> PMID: 28360091
57. Thimme R, Bukh J, Spangenberg HC, Wieland S, Pemberton J, Steiger C, et al. Viral and immunological determinants of hepatitis C virus clearance, persistence, and disease. *Proc Natl Acad Sci*. 2002 99(24):15661–8. <https://doi.org/10.1073/pnas.202608299> PMID: 12441397
58. Foupouapouognigni Y, Sadeuh Mba SA, a Betsem EB, Rousset D, Froment A, Gessain A, et al. Hepatitis B and C virus infections in the three Pygmy groups in Cameroon. *J Clin Microbiol*. 2011 49(2):737–40. <https://doi.org/10.1128/JCM.01475-10> PMID: 21106785
59. Njouom R, Pasquier C, Ayouba A, Gessain A, Froment A, Mfoupouendoun J, et al. High rate of hepatitis C virus infection and predominance of genotype 4 among elderly inhabitants of a remote village of the rain forest of South Cameroon. *J Med Virol*. 2003 71(2):219–25. <https://doi.org/10.1002/jmv.10473> PMID: 12938196
60. Obajemu AA, Rao N, Dilley KA, Vargas JM, Sheikh F, Donnelly RP, et al. IFN λ 4 attenuates antiviral responses by enhancing negative regulation of IFN signalling. *J Immunol*. 2017 199(11):3808–3820. <https://doi.org/10.4049/jimmunol.1700807> PMID: 29070670
61. Piehler J, Roisman LC, Schreiber G. New structural and functional aspects of the type I interferon-receptor interaction revealed by comprehensive mutational analysis of the binding interface. *J Biol Chem*. 2000 275(51):40425–33. <https://doi.org/10.1074/jbc.M006854200> PMID: 10984492
62. Piehler J, Thomas C, Garcia KC, Schreiber G. Structural and dynamic determinants of type I interferon receptor assembly and their functional interpretation. *Immunol Rev*. 2012 250(1):317–34. <https://doi.org/10.1111/imr.12001> PMID: 23046138
63. Trapnell C, Roberts A, Goff L, Pertea G, Kim D, Kelley DR, et al. Differential gene and transcript expression analysis of RNA-seq experiments with TopHat and Cufflinks. *Nat Protoc*. 2012 7(3):562–78. <https://doi.org/10.1038/nprot.2012.016> PMID: 22383036
64. Ran FA, Hsu PD, Wright J, Agarwala V, Scott D a, Zhang F. Genome engineering using the CRISPR-Cas9 system. *Nat Protoc*. 2013 8(11):2281–308. <https://doi.org/10.1038/nprot.2013.143> PMID: 24157548
65. Donald CL, Brennan B, Cumberworth SL, Rezelj V V., Clark JJ, Cordeiro MT, et al. Full genome sequence and sfRNA interferon antagonist activity of Zika virus from Recife, Brazil. *PLoS Negl Trop Dis*. 2016 10(10):e0005048. <https://doi.org/10.1371/journal.pntd.0005048> PMID: 27706161
66. Pietschmann T, Kaul A, Koutsoudakis G, Shavinskaya A, Kallis S, Steinmann E, et al. Construction and characterization of infectious intragenotypic and intergenotypic hepatitis C virus chimeras. *Proc Natl Acad Sci*. 2006 103(19):7408–13. <https://doi.org/10.1073/pnas.0504877103> PMID: 16651538
67. Lindenbach BD, Evans MJ, Syder AJ, Wölk B, Tellinghuisen TL, Liu CC, et al. Complete replication of hepatitis C virus in cell culture. *Science*. 2005 309(5734):623–6. <https://doi.org/10.1126/science.1114016> PMID: 15947137

68. Cowton VM, Angus AGN, Cole SJ, Markopoulou CK, Owsianka A, Dunlop JI, et al. Role of conserved E2 residue W420 in receptor binding and hepatitis C virus infection. *J Virol.* 2016 90(16):7456–68. <https://doi.org/10.1128/JVI.00685-16> PMID: 27279607
69. Domingues P, Bamford CGG, Boutell C, McLauchlan J. Inhibition of hepatitis C virus RNA replication by ISG15 does not require its conjugation to protein substrates by the HERC5 E3 ligase. *J Gen Virol.* 2015 96(11):3236–42. <https://doi.org/10.1099/jgv.0.000283> PMID: 26361997
70. Bigger C, Guerra B, Brasky K. Intrahepatic gene expression during chronic hepatitis C virus infection in chimpanzees. *J Virol.* 2004 78(24):13779–92. <https://doi.org/10.1128/JVI.78.24.13779-13792.2004> PMID: 15564486
71. Robinson MW, Aranday-Cortes E, Gatherer D, Swann R, Liefhebber JMP, Filipe ADS, et al. Viral genotype correlates with distinct liver gene transcription signatures in chronic hepatitis C virus infection. *Liver Int.* 2015 35(10):2256–64. <https://doi.org/10.1111/liv.12830> PMID: 25800823
72. Francioli LC, Menelaou A, Pulit SL, van Dijk F, Palamara PF, Elbers CC, et al. Whole-genome sequence variation, population structure and demographic history of the Dutch population. *Nat Genet.* 2014 46(8):818–25. <https://doi.org/10.1038/ng.3021> PMID: 24974849